Nonlinear Bell inequality for macroscopic measurements

Adam Bene Watts, $^{1,\,*}$ Nicole Yunger Halpern, $^{2,\,3,\,4,\,\dagger}$ and Aram Harrow $^{1,\,\ddagger}$

¹Center for Theoretical Physics, Massachusetts Institute of Technology, Cambridge, Massachusetts 02139, USA

²ITAMP, Harvard-Smithsonian Center for Astrophysics, Cambridge, MA 02138, USA

³Department of Physics, Harvard University, Cambridge, MA 02138, USA

⁴Research Laboratory of Electronics, Massachusetts Institute of Technology, Cambridge, Massachusetts 02139, USA

(Dated: May 25, 2021)

The correspondence principle suggests that quantum systems grow classical when large. Classical systems cannot violate Bell inequalities, as entanglement can. Still, limited Bell-type inequalities have been proved for certain large-scale systems. We generalize and simplify these results, proving a nonlinear Bell inequality for macroscopic measurements. Our construction requires only bipartite measurements of extensive observables that have clear physical significances, governs fermions and bosons, and is robust with respect to errors whose variances scale as the system size. The result relies on limitations on particles' interactions. A product of singlets violates the inequality. Experimental tests are feasible for photons, solid-state systems, atoms, and trapped ions. We operationalize the inequality as a nonlocal game whose players' probability of winning is not averaged over questions. Consistently with known results, violations of our Bell inequality cannot disprove local hidden-variables theories. By rejecting the disproof goal, we show, one can certify nonclassical correlations under reasonable experimental assumptions.

Can large systems exhibit nonclassical behaviors? The correspondence principle suggests not. Yet experiments are pushing the quantum-classical boundary to larger scales [1–6]: Double-slit experiments have revealed interference of fullerene wave functions and of organic molecules' wave functions [1, 4]. A micron-long mechanical oscillator's quantum state has been squeezed [5]. Many-particle systems have given rise to nonlocal correlations [7–9].

Nonlocal correlations are detected with Bell tests. In a Bell test, systems are prepared, separated, and measured in each of many trials. The outcome statistics may violate a Bell inequality. If they do, they cannot be modeled with classical physics, in the absence of loopholes.

Bell inequalities have been proved for settings that involve large scales [9–25]; see [26, 27] for reviews. These works have enhanced our understanding of the correspondence principle. Yet a large-scale Bell inequality has yet to meet, according to our knowledge, all the desirable criteria that emerge from the review [26]: bipartite (being simpler than multipartite) measurements of macroscopic observables that have clear physical significances, violations by easy-to-prepare quantum states, and sufficient generality to govern bosons and fermions.

We derive a Bell inequality that meets all these criteria. The inequality is violated by a product of N singlets, which has been prepared with photons [28], solid-state systems [29], atoms [30, 31], and trapped ions [32]. Violation of the inequality implies nonlocality if and only if pairs of particles are prepared approximately independently. Pairs' independence is assumed also in [33–35] but may be difficult to guarantee. Because of this as-

sumption, violations of our inequality do not disprove local hidden-variables theories (LHVTs), as no macroscopic system can [33–35]. By forfeiting the goal of a disproof, we show, one can certify entanglement under reasonable experimental assumptions. This certification is device-independent, requiring no knowledge of the state or experimental apparatuses, apart from particle-pair independence. Furthermore, our inequality is robust with respect to errors, including violations of the independence assumption, whose variances scale as N.

Aside from being easily testable with platforms known to produce Bell pairs, our inequality can illuminate whether poorly characterized systems harbor entanglement. Such tests would be more challenging but offer greater potential payoffs. Possible applications include Posner molecules [36–39] and cosmological systems simulated with tabletop experiments [40].

The rest of this paper is organized as follows. We introduce the setup in Sec. I. Section II contains the main results: We present and prove the Bell inequality for macroscopic measurements, using the covariance formulation of a microscopic Bell inequality [41]. Section III contains a discussion: We compare quantum correlations and global classical correlations as resources for violating our inequality, present strategies for combatting experimental noise, reconcile violations of the inequality with the correspondence principle [33–35], recast the Bell inequality as a nonlocal game, discuss a potential application to Posner molecules [36–39], and detail opportunities.

I. SETUP

Consider an experimentalist Alice who has a system A and an experimentalist Bob who has a disjoint system B. Each system consists of N microscopic subsystems,

^{*} abenewat@mit.edu

[†] nicoleyh@g.harvard.edu

[‡] aram@mit.edu

indexed with i. The ith subsystem of A can interact with the ith subsystem of B but with no other subsystems. Our setup resembles that in [33].

Alice can measure her system with settings x=0,1, and Bob can measure his system with settings y=0,1. Each microscopic subsystem reports one of two outcomes, 0 or 1. The experimentalist observes the sum of the microscopic outcomes, the value of a macroscopic random variable. Measuring A with setting x yields the macroscopic random variable A_x . B_y is defined analogously.

We will often illustrate with two beams of photons. The polarization of each photon in beam A is entangled with the polarization of a photon in beam B and vice versa. Such beams can be produced through spontaneous parametric down-conversion (SPDC) [42]: A laser beam strikes a nonlinear crystal. Upon absorbing a photon, the crystal emits two photons entangled in the polarization domain: $\frac{1}{\sqrt{2}}(|H,V\rangle + e^{i\alpha}|V,H\rangle)$. Horizontal and vertical polarizations are denoted by $|H\rangle$ and $|V\rangle$. The relative phase depends on some $\alpha \in \mathbb{R}$. The photons enter different beams. Each experimentalist measures his/her beam by passing it through a polarizer, then measuring the intensity. The measurement setting (Alice's x or Bob's y) determines the polarizer's angle. A photon passing through the polarizer yields a 1 outcome. The intensity measurement counts the 1s.

The randomness in the A_x 's and B_y 's is of three types:

- (i) Quantum randomness: If the systems are quantum, outcomes are sampled according to the Born rule during wave-function collapse.
- (ii) Local classical randomness: Randomness may taint the preparation of each AB pair of subsystems. In the SPDC example, different photons enter the crystal at different locations. Suppose that the crystal's birefringence varies over short length scales. Different photon pairs will acquire different relative phases $e^{i\alpha}$ [42].
- (iii) Global classical randomness: Global parameters that affect all the particle pairs can vary from trial to trial. In the photon example, Alice and Bob can switch on the laser; measure their postpolarizer intensities several times, performing several trials, during a time T; and then switch the laser off. The laser's intensity affects the A_x 's and B_y 's and may fluctuate from trial to trial.

Quantum randomness and global classical randomness can violate our macroscopic Bell inequality. Assuming a cap on the amount of global classical randomness, we conclude that violations imply nonclassicality. Local classical randomness can conceal violations achievable by quantum systems ideally. Local classical randomness also produces limited correlations, which we bound in our macroscopic Bell inequality. We quantify classical randomness with a noise variable r below.

Systems A and B satisfy two assumptions:

- (a) A and B are do not interact with each other while being measured. Neither system has information about the setting with which the other system is measured.
- (b) Global classical correlations are limited, as quantified in Ineq. (2).

Assumption (a) is standard across Bell inequalities. In the photon example, the beams satisfy (a) if spatially separated while passing through the polarizers and undergoing intensity measurements.

Assumption (b) is the usual assumption that parameters do not fluctuate too much between trials, due to a separation of time scales. Consider the photon example in item (ii) above. Let t denote the time required to measure the intensity, to perform one trial. The trial time must be much shorter than the time over which the global parameters drift (e.g., the laser intensity drifts): $t \gg T$. The greater the time scales' separation, the closer the system comes to satisfying assumption (b). (b) has appeared in other studies of nonclassical correlations in macroscopic systems (e.g., [33, 35]).

We fortify our Bell test by allowing for small global correlations and limited measurement precision. Both errors are collected in one parameter, defined as follows. In the absence of errors, A_x and B_y equal ideal random variables A_x' and B_y' . Each ideal variable equals a sum of independent random variables. We model the discrepancies between ideal and actual with random variables r, as in

$$A_x = A_x' + r_{A_x}. (1)$$

Our macroscopic Bell inequality is robust with respect to errors of bounded variance:

$$Var\left(r_{A_x}\right) \le \epsilon N,\tag{2}$$

wherein $\epsilon > 0$. Errors r_{B_y} are defined analogously. They obey Ineq. (2) with the same ϵ . Strategies for mitigating errors are discussed in Sec. III.

Our macroscopic Bell inequality depends on the covariances of the A_x 's and B_y 's. The covariance of random variables X and Y is defined as

$$Cov(X,Y) := \mathbb{E}([X - \mathbb{E}(X)][Y - \mathbb{E}(Y)]), \quad (3)$$

wherein $\mathbb{E}(X)$ denotes the expectation value of X. One useful combination of covariances, we define as the

macroscopic Bell parameter:¹

$$\mathcal{B}(A_0, A_1, B_0, B_1) := \frac{4}{N} [\operatorname{Cov}(A_0, B_0) + \operatorname{Cov}(A_0, B_1) + \operatorname{Cov}(A_1, B_0) - \operatorname{Cov}(A_1, B_1)].$$
(4)

II. MAIN RESULTS

We present the nonlinear macroscopic Bell inequality and sketch the proof, detailed in App. B. Then, we show how to violate the inequality using quantum systems.

Theorem 1 (Nonlinear Bell inequality for macroscopic measurements). Let systems A and B, and measurement settings x and y, be as in Sec. I. Assume that the systems are classical. The macroscopic random variables satisfy the macroscopic Bell inequality

$$\mathcal{B}(A_0, A_1, B_0, B_1) \le 16/7 + 16\epsilon + 32\sqrt{\epsilon}.$$
 (5)

Proof. Here, we prove the theorem when $\epsilon=0$, when the observed macroscopic random variables A_x and B_y equal the ideal A_x' and B_y' . The full proof is similar but requires an error analysis (App. B).

Let $a_x^{(i)}$ denote the value reported by the $i^{\rm th}$ A particle after A is measured with setting x. A_x' and B_y' equal sums of the microscopic variables:

$$A'_{x} = \sum_{i=1}^{N} a_{x}^{(i)}, \text{ and } B'_{x} = \sum_{i=1}^{N} b_{x}^{(i)}.$$
 (6)

Because $a_0^{(i)}$ and $b_0^{(i)}$ are independent of the other variables,

$$Cov(A'_0, B'_0) = \sum_{i=1}^{N} Cov(a_0^{(i)}, b_0^{(i)}).$$
 (7)

Analogous equalities govern the other macroscopic-random-variable covariances.

Let us bound the covariances amongst the $a_x^{(i)}$'s and $b_y^{(i)}$'s. We use the covariance formulation of the Bell-Clauser-Horne-Shimony-Holt (Bell-CHSH) inequal-

ity (see [41, 43] and App. C),²

$$\operatorname{Cov}\left(a_0^{(i)}, b_0^{(i)}\right) + \operatorname{Cov}\left(a_0^{(i)}, b_1^{(i)}\right) + \operatorname{Cov}\left(a_1^{(i)}, b_0^{(i)}\right) - \operatorname{Cov}\left(a_1^{(i)}, b_1^{(i)}\right) \le 4/7. \quad (8)$$

Combining Eq. (7) and Ineq. (8) with the definition of $\mathcal{B}(A'_x, A'_y, B'_x, B'_y)$ [Eq. (4)] gives

$$\mathcal{B}(A_0', A_1', B_0', B_1') = \frac{4}{N} \sum_{i=1}^{N} \left[\text{Cov} \left(a_0^{(i)}, b_0^{(i)} \right) \right]$$
 (9)

+
$$\operatorname{Cov}\left(a_0^{(i)}, b_1^{(i)}\right) + \operatorname{Cov}\left(a_1^{(i)}, b_0^{(i)}\right) - \operatorname{Cov}\left(a_1^{(i)}, b_1^{(i)}\right)\right] \le 16/7.$$
 (10)

We now show that a quantum system can produce correlations that violate Ineq. (5). The system consists of singlets.

Theorem 2. There exist an N-particle quantum system and a measurement strategy, subject to the restrictions in Sec. I, whose outcome statistics violate the nonlinear Bell inequality for macroscopic measurements. The system and strategy achieve

$$\mathcal{B}(A_0, A_1, B_0, B_1) = 2\sqrt{2} \tag{11}$$

in the ideal ($\epsilon = 0$) case and

$$\mathcal{B}(A_0, A_1, B_0, B_1) \ge 2\sqrt{2} - 16\epsilon - 32\sqrt{\epsilon} \tag{12}$$

in the presence of noise bounded as in Ineq. (2).

Proof. As in the proof of Theorem 1, we prove the result in the ideal case here. Appendix D contains the error analysis. Let each of A and B consist of N qubits. Let the i^{th} qubit of A and the i^{th} qubit of B form a singlet, for all $i\colon |\Psi^-\rangle:=\frac{1}{\sqrt{2}}(|01\rangle-|10\rangle)$. We denote the 1 and -1 eigenstates of the Pauli z-operator σ_z by $|0\rangle$ and $|1\rangle$. Let x and y be the measurement settings in the conventional CHSH test ([43], reviewed in App. C). If the measurement of a particle yields 1, the particle effectively reports 1; and if the measurement yields -1, the particle reports 0.

Measuring the $i^{\rm th}$ particle pair yields outcomes that satisfy

$$\mathbb{E}\left(a_0^{(i)}\right) = \mathbb{E}\left(a_1^{(i)}\right) = \mathbb{E}\left(b_0^{(i)}\right) = \mathbb{E}\left(b_1^{(i)}\right) = \frac{1}{2}. \quad (13)$$

Calculating \mathcal{B} requires knowledge of N, the number of particles in each experimentalist's system. N might not be measurable precisely. But knowing N even to within \sqrt{N} suffices: Taylorapproximating yields $\frac{1}{N+\sqrt{N}}=\frac{1}{N}\left(1-\frac{1}{\sqrt{N}}\right)$. The correction is of size $\frac{1}{\sqrt{N}}\ll 1$. Furthermore, uncertainty about N may be incorporated into a noise model with which a macroscopic Bell inequality can be derived (App. A).

 $^{^2}$ In the original statement of Ineq. (8), the right-hand side (RHS) equals 16/7. The reason is, in [41], $a_x^{(i)}$, $b_y^{(i)} \in [-1,1]$. We assume that each variable $\in [0,1]$, so we deform the original result in two steps. First, we translate [-1,1] to [0,2]. Translations preserve covariances. Second, we rescale [0,2] to [0,1]. The rescaling halves each a and b, quartering products ab, the covariances, and the 16/7 in Ineq. (8). The resulting 4/7 is multiplied by a 4 in Ineq. (9), returning to 16/7.

As shown in App. D,

$$\mathbb{E}\left(a_0^{(i)}b_0^{(i)}\right) + \mathbb{E}\left(a_0^{(i)}b_1^{(i)}\right)$$

$$+ \mathbb{E}\left(a_1^{(i)}b_0^{(i)}\right) - \mathbb{E}\left(a_1^{(i)}b_1^{(i)}\right) = 2\sin^2(3\pi/8) - \frac{1}{2}.$$
(14)

Combining these two equations yields

$$\operatorname{Cov}\left(a_0^{(i)}, b_0^{(i)}\right) + \operatorname{Cov}\left(a_0^{(i)}, b_1^{(i)}\right) \tag{15}
+ \operatorname{Cov}\left(a_1^{(i)}, b_0^{(i)}\right) - \operatorname{Cov}\left(a_1^{(i)}, b_1^{(i)}\right) = 2\sin^2(3\pi/8) - 1.
= 1/\sqrt{2}. \tag{16}$$

Following the proof of Theorem 1, we compute

$$\mathcal{B}(A'_0, A'_1, B'_0, B'_1) \tag{17}$$

$$= \frac{4}{N} \sum_{i} \left[\text{Cov} \left(a_0^{(i)}, b_0^{(i)} \right) + \text{Cov} \left(a_0^{(i)}, b_1^{(i)} \right) + \text{Cov} \left(a_1^{(i)}, b_0^{(i)} \right) - \text{Cov} \left(a_1^{(i)}, b_1^{(i)} \right) \right] \tag{18}$$

$$= 2\sqrt{2}. \tag{19}$$

III. DISCUSSION

Six points merit analysis. First, we discuss the equivalence of local quantum correlations and global classical correlations as resources for violating the macroscopic Bell inequality. Second, we suggest strategies for mitigating experimental errors. Third, we reconcile our macroscopic-Bell-inequality violation with the principle of macroscopic locality, which states that macroscopic systems should behave classically [33–35]. Fourth, we recast our macroscopic Bell inequality in terms of a non-local game. Fifth, we discuss a potential application to the Posner model of quantum cognition [36–39]. Sixth, we detail opportunities engendered by this work.

Violating the macroscopic Bell inequality with classical global correlations: Violating the inequality (5) is a quantum information-processing (QI-processing) task. Entanglement fuels some QI-processing tasks equivalently to certain classical resources (e.g., [44]). In violating the macroscopic Bell inequality, entanglement within independent particle pairs serves equivalently to global classical correlations. We prove this claim in App. E. The reason is the inequality's nonlinearity in the probabilities according to which the A_x 's and B_y 's are distributed. This result elucidates entanglement's power in QI processing.

Two strategies for mitigating experimental imperfections: Imperfections generate local classical (ii) and global classical (iii) randomness, discussed in Sec. I. Local classical randomness can conceal quantum violations of the macroscopic Bell inequality, making the macroscopic Bell parameter \mathcal{B} (4) appear smaller than

it should. Global classical randomness can lead classical systems to violate the inequality. These effects can be mitigated in two ways.

First, we can reduce the effects of local classical randomness on \mathcal{B} by modeling noise more precisely than in Sec. I. A macroscopic Bell inequality tighter than Ineq. (5) may be derived. We illustrate in App. A, with noise that acts on the microscopic random variables $a_x^{(i)}$ and $b_y^{(i)}$ independently. Second, we can mitigate global classical randomness by reinitializing global parameters between trials. In the photon example, the laser can be reset between measurements.

Reconciliation with the principle of macroscopic locality: Macroscopic locality has been proposed as an axiom for distinguishing quantum theory from other nonclassical probabilistic theories [33–35] (see [45, 46] for a more restrictive proposal). Suppose that macroscopic properties of N independent quantum particles are measured with precision $\sim \sqrt{N}$. The outcomes are random variables that obey a probability distribution P. A LHVT can account for P, according to the principle of macroscopic locality.

The violation of our macroscopic Bell inequality would appear to violate the principle of macroscopic locality. But experimentalists cannot guarantee the absence of fluctuating global parameters, no matter how tightly they control the temperature, laser intensity, etc. Some unknown global parameter could underlie the Bellinequality violation, due to the inequality's nonlinearity. This parameter would be a classical, and so local, hidden variable. Hence violating our macroscopic Bell inequality does not disprove LHVTs. Rather, a violation signals nonlocal correlations under reasonable, if not airtight, assumptions about the experiment (Sec. I).

Nonlocal game: The macroscopic Bell inequality gives rise to a nonlocal game. Nonlocal games quantify what quantum resources can achieve that classical resources cannot. The CHSH game is based on the Bell-CHSH inequality ([43, 47, 48] and App. C): Players Alice and Bob agree on a strategy; share a resource, which might be classical or quantum; receive questions x and y from a verifier; operate on their particles locally; and reply with answers a_x and b_y . If the questions and answers satisfy $x \wedge y = a + b \pmod{2}$, the players win. Players given quantum resources can win more often than classical players can.

Our macroscopic game (App. F) resembles the CHSH game but differs in several ways: N Alices and N Bobs play. The verifier aggregates the Alices' and Bobs' responses, but the verifier's detector has limited resolution. The aggregate responses are assessed with a criterion similar to the CHSH win condition. After many rounds of the game, the verifier scores the player's performance. The score involves no averaging over all possible question pairs xy. Players who share pairwise entanglement (such that each Alice shares entanglement with only one Bob and vice versa) can score higher than classical players.

Toy application to Posner molecules: Fisher has

proposed a mechanism by which entanglement might enhance coordinated neuron firing [36]. Phosphorus nuclear spins, he argues, can retain coherence for long times when in Posner molecules $\text{Ca}_9(\text{PO}_4)_6$ [49–55]. (We call Posner molecules "Posners" for short.) He has argued that Posners might share entanglement. Fisher's work has inspired developments in quantum computation [38, 56], chemistry [37, 55], and many-body physics [57–59]. The experimental characterization of Posners has begun. If long-term coherence is observed, entanglement in Posners should be tested for.

How could it be? Posners tumble randomly in their room-temperature fluids. In Fisher's model, Posners can undergo the quantum-computational operations detailed in [38], not the measurements performed in conventional Bell tests. Fisher sketched an inspirational start to an entanglement test in [39]. Concretizing the test as a nonlocal game was proposed in [38]. We initiate the concretization in App. G. Our Posner Bell test requires microscopic control but proves that Posners can violate a Bell inequality, in principle, in Fisher's model. Observing such a violation would require more experimental effort than violating our inequality with photons. But a Posner violation would signal never-before-seen physics: entanglement amongst biomolecules.

Opportunities: This work opens up four avenues of research. First, violations of our inequality can be observed experimentally. Potential platforms include photons [28], solid-state systems [29], atoms [30, 31], and trapped ions [32]. These systems could be conscripted relatively easily but are known to generate nonclassical correlations. More ambitiously, one could test our macroscopic Bell inequality with systems whose nonclassicality needs characterization. Examples include the cosmic microwave background (CMB) and Posner molecules. Detecting entanglement in the CMB faces difficulties: Some

of the modes expected to share entanglement have such suppressed amplitudes, they cannot be measured [60]. Analogs of cosmological systems, however, can be realized in tabletop experiments [40]. Such an experiment's evolution can be paused. Consider pausing the evolution before, or engineering the evolution to avoid, the suppression. From our Bell test, one might infer about entanglement in the CMB. A Posner application would require the elimination of microscopic control from the Bell test in App. G, opportunity two.

Third, the greatest possible macroscopic Bell parameter \mathcal{B} achievable by any quantum system merits identification. This upper bound would serve as a quantum nonlinear Bell inequality [34, 61–63]. Which quantum state achieves the bound would further illuminate nonclassical correlations.

Fourth, which macroscopic Bell parameters \mathcal{B} can probabilistic theories beyond quantum theory realize? Other theories can support correlations unrealizable in quantum theory [64, 65]. These opportunities can help distinguish quantum theory from alternative physics while illuminating the quantum-to-classical transition.

ACKNOWLEDGMENTS

The authors thank Isaac Chuang, Alan Guth, David I. Kaiser, Christopher McNally, Robert W. Spekkens, and John Wright for helpful discussions. We acknowledge inspiration from talks by Matthew Fisher, and we thank Elizabeth Crosson for sharing code. ABW was funded by NSF grant CCF-1729369. NYH is grateful for an NSF grant for the Institute for Theoretical Atomic, Molecular, and Optical Physics at Harvard University and the Smithsonian Astrophysical Observatory. AWH was funded by NSF grants CCF-1452616, CCF-1729369, PHY-1818914 and ARO contract W911NF-17-1-0433.

Appendix A EXAMPLE NOISE MODEL

The bounds presented in Theorems 1 and 2 are worst-case bounds. They hold for any noise that satisfies the variance bounds of Eq. 2. However, experimental assumptions can often constrain noise further. A noise-specific analysis can lead to bounds that separate classical from nonclassical correlations when the general bounds cannot. We illustrate with noise that acts on the microscopic random variables independently.

For concreteness, we analyze errors that occur when photon beams are produced via SPDC (Sec. I). We do this for two reasons. First, we hope to demonstrate that a macroscopic Bell test is physically viable. Second, ideas in this analysis may generalize to other physical setups. This section will provide a template for device-specific noise analysis.

We begin by reviewing the setup. Photon beams are produced when a laser shines on a nonlinear crystal. The crystal down-converts some fraction of the incident photons: Upon absorbing one photon, the crystal emits two. The two photons travel in different paths, and their polarizations become maximally entangled. If this process occurs frequently enough,³ two distinct beams of photons, whose polarizations form Bell states, result.

This process can involve two sources of randomness. First, imagine placing a perfect-efficiency detector right next to the crystal, in the path of one of the beams. The detector's clicking rate is expected to obey a Poisson distribution. The distribution governs the number of photon pairs produced by the crystal per unit time. This number is a random

³ Coincidence rates of ≈ 10 per second were reported in [42].

variable whose randomness is global and classical, or is of type (iii) (Sec. I). Second, photons can be lost between being produced in the crystal and being measured by Alice's or Bob's post-polarization detector. Dust on the polarizer could absorb a photon, for example, or the detector could have subunit efficiency. This randomness is local and classical, or of type (ii). We model the randomness of both types, then use the model to prove tighter analogs of Theorems 1 and 2.

Our first step in tightening the classical bound (Theorem 1) is to identify the most general form that the macroscopic random variables A_0 , A_1 , B_0 , and B_1 can assume. Let M be the number of photons in the laser beam that strikes the crystal (per unit time). We call these "incident photons." Assume that each incident photon down-converts with probability λ , independently of the other possible down-conversions.⁴ The total number of photon pairs produced is represented by a random variable $\sum_{i=1}^{M} e_i$. The e_i 's are independent Bernoulli random variables, each with mean λ . Down-conversion is improbable [66], so λ is small: $\lambda \ll 1$.

The random variable $a_x^{(i)}$ describes the value that would be reported if the i^{th} incident photon participated in a down-conversion event and the resultant photon in Alice's beam were measured with measurement setting x. The random variable $b_y^{(i)}$ is defined analogously. The i^{th} possible down-conversion event can add a photon to Alice's beam. Suppose that Alice measures with setting x. Whether that photon is lost before detection is represented by $l_{a,x}^{(i)}$. This random variable equals 0 if the photon is lost and equals 1 otherwise. The random variable $l_{b,y}^{(i)}$ is defined analogously. These variables govern the macroscopic random variables:

$$A_x = \sum_{i=1}^{M} e_i a_x^{(i)} l_{a,x}^{(i)}, \quad \text{and} \quad B_y = \sum_{i=1}^{M} e_i b_y^{(i)} l_{b,y}^{(i)}.$$
(A1)

How the total particle number, N, should be defined is ambiguous. Several possibilities suggest themselves. We choose a definition that leads to strong bounds: In the ideal quantum experiment in Sec. II, each microscopic random variable has a probability 1/2 of reporting 1 and a probability 1/2 of reporting 0. Hence $\mathbb{E}(A_0) = \mathbb{E}(A_1) = \mathbb{E}(B_0) = \mathbb{E}(B_1) = N/2$. We turn this observation into a definition:

$$N = \mathbb{E}(A_0) + \mathbb{E}(B_0). \tag{A2}$$

Proceeding from definitions to bounds, we compute the macroscopic random variables' covariances. For all $x, y \in \{0, 1\}$,

$$Cov(A_x, B_y) = \sum_{i=1}^{M} Cov\left(e_i a_x^{(i)} l_{a,x}^{(i)}, e_i b_y^{(i)} l_{b,y}^{(i)}\right)$$
(A3)

$$= \sum_{i=1}^{M} \left[\mathbb{E} \left(e_i a_x^{(i)} l_{a,x}^{(i)} b_y^{(i)} l_{b,y}^{(i)} \right) - \mathbb{E} \left(e_i a_x^{(i)} l_{a,x}^{(i)} \right) \mathbb{E} \left(e_i b_y^{(i)} l_{b,y}^{(i)} \right) \right]$$
(A4)

$$= \sum_{i=1}^{M} \left[\lambda \mathbb{E} \left(a_x^{(i)} l_{a,x}^{(i)} b_y^{(i)} l_{b,y}^{(i)} \right) - \lambda^2 \mathbb{E} \left(a_x^{(i)} l_{a,x}^{(i)} \right) \mathbb{E} \left(b_y^{(i)} l_{b,y}^{(i)} \right) \right]$$
(A5)

$$= \lambda \sum_{i=1}^{M} \mathbb{E}\left(a_x^{(i)} l_{a,x}^{(i)} b_y^{(i)} l_{b,y}^{(i)}\right) + O(M\lambda^2). \tag{A6}$$

The macroscopic random variables have averages of the form

$$\mathbb{E}(A_x) = \sum_{i=1}^{M} \mathbb{E}\left(e_i a_x^{(i)} l_{a,x}^{(i)}\right) = \lambda \sum_{i=1}^{M} \mathbb{E}\left(a_x^{(i)} l_{a,x}^{(i)}\right). \tag{A7}$$

Substituting into Eq. (4), we form the macroscopic Bell parameter:

$$\mathcal{B}(A_0, A_1, B_0, B_1) = \frac{4\sum_{i=1}^{M} \left[\lambda \mathbb{E} \left(a_0^{(i)} l_{a,0}^{(i)} b_0^{(i)} l_{b,0}^{(i)} + a_0^{(i)} l_{a,0}^{(i)} b_1^{(i)} l_{b,1}^{(i)} + a_1^{(i)} l_{a,1}^{(i)} b_0^{(i)} l_{b,0}^{(i)} - a_1^{(i)} l_{a,1}^{(i)} b_1^{(i)} l_{b,1}^{(i)} \right) \right] + O(M\lambda^2)}{\lambda \sum_{i=1}^{M} \mathbb{E} \left(a_0^{(i)} l_{a,0}^{(i)} + b_0^{(i)} l_{b,0}^{(i)} \right)}.$$
(A8)

conversion time scale. Small deviations from this assumption can be accommodated with the bound in App. B.

We are assuming that the possible down-conversions are independent. This assumption can be approximately satisfied if the time scale over which global parameters change ≫ the down-

We will bound the RHS under the assumption that the microscopic variables are classical. Then, we will show that the bound can be violated with a quantum state.

Classical bound: We bound the numerator of Ineq. (A8) using a general inequality. For any variables $a_0, a_1, b_0, b_1 \in \{0, 1\}$,

$$a_0b_0 + a_0b_1 + a_1b_0 - a_1b_1 \le a_0 + b_0. \tag{A9}$$

Let $a_x = a_x^{(i)} l_{a,x}^{(i)}$ and $b_y = b_y^{(i)} l_{b,y}^{(i)}$. Applying Ineq. (A9) to the numerator of Ineq. (A8) yields

$$\mathbb{E}\left(a_0^{(i)}l_{a,0}^{(i)}b_0^{(i)}l_{b,0}^{(i)} + a_0^{(i)}l_{a,0}^{(i)}b_1^{(i)}l_{b,1}^{(i)} + a_1^{(i)}l_{a,1}^{(i)}b_0^{(i)}l_{b,0}^{(i)} - a_1^{(i)}l_{a,1}^{(i)}b_1^{(i)}l_{b,1}^{(i)}\right) \le \mathbb{E}\left(a_0^{(i)}l_{a,0}^{(i)} + b_0^{(i)}l_{b,0}^{(i)}\right). \tag{A10}$$

We substitute into the numerator in Ineq. (A8), then cancel the $\mathbb{E}(...)$ in the denominator. The classical macroscopic random variables satisfy⁵

$$\mathcal{B}(A_0, A_1, B_0, B_1) \le 4 + O(M\lambda^2/N). \tag{A11}$$

We can understand this result as follows. The randomness in N serves as noise. It raises the macroscopic Bell bound (A11) above the main-text macroscopic Bell bound (5) and even above the quantum bound (12). In this setting, however, a quantum bound lies above the classical (A11).

Quantum violation of the classical bound: We can relax our assumptions, because experiments will replace this calculation. Once experimentalists observe covariances that violate Ineq. (5) or Ineq. (A11), they can conclude that the particles are nonclassical, if the global correlations are small enough to be unlikely to have caused the violation. The experimentalists need not worry about precisely why the violation occurred.

We therefore simplify by assuming that $l_{a,0}$, $l_{a,1}$, $l_{b,0}$, and $l_{b,1}$ obey Bernoulli distributions with the same mean, γ . The macroscopic Bell parameter becomes

$$\mathcal{B}(A_0, A_1, B_0, B_1) = \frac{4\sum_{i=1}^{M} \left[\gamma \mathbb{E} \left(a_0^{(i)} b_0^{(i)} + a_0^{(i)} b_1^{(i)} + a_1^{(i)} b_0^{(i)} - a_1^{(i)} b_1^{(i)} \right) + O(\lambda) \right]}{\sum_{i=1}^{M} \mathbb{E} \left(a_0^{(i)} + b_0^{(i)} \right)}.$$
(A12)

If the experimentalists follow the quantum strategy in Sec. II, the microscopic random variables satisfy [Eq. (14)]

$$\mathbb{E}\left(a_0^{(i)}b_0^{(i)} + a_0^{(i)}b_1^{(i)} + a_1^{(i)}b_0^{(i)} - a_1^{(i)}b_1^{(i)}\right) = 2\sin^2(3\pi/8) - 1/2 \tag{A13}$$

and [Eq. (13)]

$$\mathbb{E}\left(a_x^{(i)} + b_x^{(i)}\right) = 1. \tag{A14}$$

We substitute into the numerator and denominator of Eq. (A12). The quantum strategy achieves a macroscopic Bell parameter of

$$\mathcal{B}(A_0, A_1, B_0, B_1) = 2\gamma [4\sin^2(3\pi/8) - 1] + O(\lambda). \tag{A15}$$

A quantum system can violate the classical bound (A11) if

$$\gamma > \frac{2 + O(M\lambda^2/N)}{4\sin^2(3\pi/8) - 1 + O(\lambda)} \approx 0.828 + O(M\lambda^2/N).$$
(A16)

Photons can violate the noise-specific macroscopic Bell inequality (A11) if $\gtrsim 83\%$ of the photon pairs created arrive at the detectors.

A similar condition arises in the standard Bell test: The standard test suffers from a detection loophole if the detector misses too many incident photons. As with the detection loophole, a Bell test remains possible here even if too many photons are lost [even if the system disobeys Ineq. (A16)]. Formulating the Bell test would require a more-detailed noise model.

the probability that a given laser-beam photon down-converts, and N denotes the number of photons in Alice or Bob's beam. Hence $N \approx \lambda M$.

⁵ The correction in Ineq. (A11) is small when Alice and Bob measure as dictated in the "Quantum violation of the classical bound" section below: The correction decomposes as $M\lambda^2/N = \left(\frac{M\lambda}{N}\right)\lambda$. The final $\lambda \ll 1$ by assumption. M denotes the number of photons in the laser beam that hits the crystal, λ denotes

Appendix B PROOF OF NONLINEAR BELL INEQUALITY FOR MACROSCOPIC MEASUREMENTS

We now prove Theorem 1 in full generality, building on the proof in Sec. II. The added analysis introduces robustness against weak global classical correlations [randomness of type (iii), according to Sec. I].

Proof. First, we review notation. Second, we bound the observed Bell correlator $\mathcal{B}(A_0, A_1, B_0, B_1)$, using (i) the ideal Bell correlator $\mathcal{B}(A_0', A_1', B_0', B_1')$ and (ii) the bound (2) on global correlations.

Recall the definitions given in Sec. II. A_0 , A_1 , B_0 , and B_1 represent the macroscopic random variables observed by the experimentalists. A'_0 , A'_1 , B'_0 , and B'_1 represent the random variables that the experimentalists would measure if all global parameters were fixed to their ideal values. In the photon example, the laser's intensity, the laser-crystal alignment, etc. would remain constant across trials. Equation (1) relates the measured variables to the ideals via the error variable r. Inequality (2) bounds the error's variance.

We aim to bound the observed correlator $\mathcal{B}(A_0, A_1, B_0, B_1)$ in terms of the ideal correlator $\mathcal{B}(A_0', A_1', B_0', B_1')$ and ϵ . Algebraic manipulation gives

$$Cov (A_x, B_y) = Cov (A'_x + r_{A_x}, B'_y + r_{B_y})$$
(B1)

$$= \operatorname{Cov}\left(A_{x}^{\prime}, B_{y}^{\prime}\right) + \operatorname{Cov}\left(A_{x}^{\prime}, r_{B_{y}}\right) + \operatorname{Cov}\left(r_{A_{x}}, B_{y}^{\prime}\right) + \operatorname{Cov}\left(r_{A_{x}}, r_{B_{y}}\right). \tag{B2}$$

Random variables X and Y have a covariance $\mathrm{Cov}(X,Y)$ bounded in terms of the variables' variances: Let $\mathcal{X} := X - \langle X \rangle$ and $\mathcal{Y} := Y - \langle Y \rangle$. The original variables have the covariance

$$Cov(X,Y) = \mathbb{E}(\mathcal{X}\mathcal{Y}) \le \sqrt{\mathbb{E}(\mathcal{X}^2)\mathbb{E}(\mathcal{Y}^2)} = \sqrt{Var(X)Var(Y)}.$$
 (B3)

The bound follows from the Cauchy-Schwarz inequality. We apply Ineq. (B3) to each of the final three covariances in Eq. (B2):

$$\left|\operatorname{Cov}\left(A_{x}, B_{y}\right) - \operatorname{Cov}\left(A_{x}', B_{y}'\right)\right| = \left|\operatorname{Cov}\left(A_{x}', r_{B_{y}}\right) + \operatorname{Cov}\left(r_{A_{x}}, B_{y}'\right) + \operatorname{Cov}\left(r_{A_{x}}, r_{B_{y}}\right)\right|$$
(B4)

$$\leq \sqrt{\operatorname{Var}(A'_{x})\operatorname{Var}(r_{B_{y}})} + \sqrt{\operatorname{Var}(r_{A_{x}})\operatorname{Var}(B'_{y})} + \sqrt{\operatorname{Var}(r_{A_{x}})\operatorname{Var}(r_{B_{y}})}$$
(B5)

$$\leq (\epsilon + 2\sqrt{\epsilon})N.$$
 (B6)

The final inequality follows from Ineq. (2) and $\operatorname{Var}(A'_x) \leq N$. This latter inequality holds because A'_x equals a sum of N independent terms $a_x^{(i)}$. Each $a_x^{(i)} \in \{0,1\}$ and so has variance ≤ 1 . We combine Ineq. (B6) with Eq. (4) and the triangle inequality to conclude that

$$|\mathcal{B}(A_0, A_1, B_0, B_1) - \mathcal{B}(A_0', A_1', B_0', B_1')| \le 16\epsilon + 32\sqrt{\epsilon}.$$
 (B7)

According to the sketch of the proof of Theorem 1 [Ineq. (10)],

$$\mathcal{B}(A_0', A_1', B_0', B_1') \le 16/7. \tag{B8}$$

Combing Ineqs. (B7) and (B8) gives

$$\mathcal{B}(A_0, A_1, B_0, B_1) \le 16/7 + 16\epsilon + 32\sqrt{\epsilon},\tag{B9}$$

the desired result.

Appendix C BACKGROUND: CHSH GAME

Before describing the CHSH game, we establish a more general framework for two-party nonlocal games. Nonlocal games illustrate how players given quantum resources can outperform players given only classical resources. A two-party nonlocal game involves two players, Alice and Bob. They share some resource—typically, classical shared randomness or a quantum state. They cannot communicate after agreeing on the strategy they will follow. The game begins when a verifier sends Alice a question, or symbol, x, and sends Bob a question y. Using only the questions and possibly measurements of the shared resource, the players respond with symbols a and b. The verifier substitutes x, y, a, and b into a function. If the function's value satisfies some predetermined criterion, the players win the game.

Every nonlocal game has a list of winning response pairs ab for every question pair xy. The players aim to maximize their probability of responding with a winning ab, knowing the winning response lists and the distribution from which the questions are drawn. The maximal win probability is called the game's value.

The CHSH game is described as follows in this language. Questions x and y are drawn from $\{0,1\}$. Winning responses are $a,b \in \{0,1\}$ such that

$$x \wedge y = a + b \pmod{2}. \tag{C1}$$

The \wedge denotes the logical AND. Table I summarizes the winning response pairs.

$$\begin{array}{c|c|c} y \backslash x & 0 & 1 \\ \hline 0 & 00 & 11 & 00 & 11 \\ 1 & 00 & 11 & 01 & 10 \\ \end{array}$$

TABLE I: Diagrammatic specification of the CHSH game: Each column corresponds to one possible value of Alice's question, x, and each row corresponds to one possible value of Bob's question, y. Each cell contains the winning response pairs ab.

The CHSH game illustrates the separation between what players can achieve when sharing only classical resources and what players can achieve when sharing entanglement. Suppose that x and y are selected uniformly randomly. Players given only classical resources have a probability $\leq 3/4$ of winning a random round. Players who measure a shared entangled state have a probability $\sin^2(3\pi/8) \approx 0.854$. Both facts are proved below.

Theorem 3. A classical strategy based on shared randomness can win the CHSH game with probability at most 3/4.

Proof. Classical players can achieve the value (the optimal win probability) with a deterministic strategy. We prove this claim with a fairly standard minimax argument: Let ω denote the game's value. Assume that some randomness-based strategy achieves ω . Let r denote the random seed. By assumption,

$$\mathbb{E}_r \left(\mathbb{E}_{a,b} \left(\sum_{a,b: x \wedge y = a + b} P(a, b \mid x, y, r) \right) \right) = \omega.$$
 (C2)

P(a, b | x, y, r) denotes the probability that the players respond with a and b, conditioned on the questions x and y and on the random seed r. Some value r_0 of r maximizes the inner expectation value, by the average's convexity. Fixing $r = r_0$ results in a deterministic strategy that achieves the game's value, ω , as claimed.

Restricted to deterministic strategies, the players have few options. Given a question i, a player must respond with some fixed output. Define a_i as Alice's response to the question i, and define b_i as Bob's response to i. In the CHSH game, the winning responses satisfy $a_i, b_i \in \{0, 1\}$,

$$a_0 + b_0 = 0 \pmod{2},$$
 (C3)
 $a_1 + b_0 = 0 \pmod{2},$ and
 $a_0 + b_1 = 0 \pmod{2},$ and
 $a_1 + b_1 = 1 \pmod{2}.$

Linear algebra over \mathbb{F}_2 shows that these equations cannot all be satisfied simultaneously. Hence any deterministic classical strategy must lose on at least one of the four question pairs. Such a strategy wins a random round with probability $\leq 3/4$.

Constructing a deterministic classical strategy that achieves a win probability of 3/4 is straightforward [47, 48]. The construction shows that the CHSH game's classical value is 3/4.

Next, we construct a quantum strategy that has a superclassical probability > 3/4 of winning the CHSH game. Our presentation is nonstandard but will prove useful later. We begin by reviewing notation and facts about maximally entangled two-qubit states.

Let $|\Psi^-\rangle := \frac{1}{\sqrt{2}} \left(|01\rangle - |10\rangle \right)$ denote the singlet and $|\Psi^-(\theta)\rangle := \frac{1}{\sqrt{2}} \left(|01\rangle - e^{i\theta}|10\rangle \right)$. We denote the operator that rotates one qubit about the z-axis through an angle θ by $R_z(\theta) := e^{-i\theta\sigma_z/2}$.

Lemma 1. Rotations compose as

1.
$$[R_z(\theta_1) \otimes R_z(-\theta_2)]|\Psi^-\rangle = (phase)|\Psi^-(\theta_1 + \theta_2)\rangle$$
.

Consider preparing a pure two-qubit state $|\psi\rangle$, then measuring $\sigma_x\otimes\sigma_x$. A classical two-bit string results. Let $P_{XX}\left(S|\psi\right)$ denote the string's probability of being in the set S. If $S_{\text{even}}:=\{00,11\}$ and $S_{\text{odd}}:=\{01,10\}$,

- 2. $P_{XX}(S_{\text{even}} | \Psi^-) = 0$,
- 3. $P_{XX}(S_{\text{even}} | \Psi^{-}(\pi)) = 1$, and
- 4. $P_{XX}(S_{\text{even}} | \Psi^{-}(\theta)) = \sin^2(\theta/2)$.

Proof. Identities 1–3 can be verified by direct calculation. To prove identity 4, we note that $|\Psi^{-}(\theta)\rangle$ equals a linear combination of $|\Psi^{-}\rangle$ and $|\Psi^{-}(\pi)\rangle$. Furthermore, $\langle\Psi^{-}|\Psi^{-}(\pi)\rangle = 0$. Hence $|\Psi^{-}(\theta)\rangle = \alpha|\Psi^{-}\rangle + \beta|\Psi^{-}(\pi)\rangle$, and

$$P_{XX}(S_{\text{even}} | \Psi^{-}(\theta)) = |\alpha|^2 = |\langle \Psi^{-} | \Psi^{-}(\theta) \rangle|^2$$
(C4)

$$= \frac{1}{4}|1 - \exp(i\theta)|^2 \tag{C5}$$

$$= \frac{1}{2} [1 - \cos(\theta)] = \sin^2(\theta/2). \tag{C6}$$

These facts underlie a strategy for winning the CHSH game, using quantum resources, with a greater probability than is achievable with only classical resources. The quantum strategy consists of the following steps:

- 1. Alice and Bob prepare $|\Psi^{-}\rangle$, and each player takes one qubit. The players agree on how each will generate a response, given any possible question.
- 2. Upon receiving question i, Alice rotates her qubit with $R_z(\theta_i)$. Upon receiving question i, Bob rotates his qubit with $R_z(-\theta_i)$. The rotation angle θ_i depends on the question and the strategy.
- 3. Each player measures his/her qubit's σ_x . The outcome is sent to the verifier as a response.

We now identify angles θ_i that lead to a superclassical probability of winning the CHSH game.

Lemma 2. A quantum strategy with rotation angles $\theta_0 = -3\pi/8$ and $\theta_1 = 9\pi/8$ wins the CHSH game with probability $\sin^2(3\pi/8) \approx 0.854$.

Proof. We verify the claim computationally. Upon receiving the question pair 00, the players win with a probability

$$P_{XX}(S_{\text{even}} | \Psi^{-}(3\pi/4)) = \sin^{2}(-3\pi/8).$$
 (C7)

Upon receiving 01 or 10, the players win with a probability

$$P_{XX}(S_{\text{even}} | \Psi^{-}(3\pi/4)) = \sin^2(3\pi/8).$$
 (C8)

Finally, upon receiving 11, the players win with a probability

$$P_{XX}(S_{\text{odd}} | \Psi^{-}(9\pi/4)) = 1 - P_{XX}(S_{\text{even}} | \Psi^{-}(9\pi/4))$$
 (C9)

$$= 1 - \sin^2(9\pi/8) \tag{C10}$$

$$=\sin^2(3\pi/8). \tag{C11}$$

Hence the players have a total win probability, averaged over the possible question pairs, of $\sin^2(3\pi/8)$.

A wide range of rotation angles can achieve superclassical win probabilities. For example, $\theta_0 = \pi/2$ and $\theta_1 = 3\pi/4$ lead to a win probability of ≈ 0.802 .

Appendix D DETAILS: QUANTUM VIOLATION OF THE NONLINEAR BELL INEQUALITY FOR MACROSCOPIC MEASUREMENTS

Here, we complete the proof of Theorem 2. In App. D 1, we prove Eq. (14). Appendix D 2 shows that the proof in the main text is robust with respect to small experimental imperfections.

D 1 Proof of Eq. (14)

Let $|\Psi^-\rangle:=\frac{1}{\sqrt{2}}(|01\rangle-|10\rangle)$ denote the singlet. We simplify notation by omitting superscripts from the microscopic responses, e.g., $a_x^{(i)}$. Recall that $a_x,b_y\in\{0,1\}$. Consequently, for any $x,y\in\{0,1\}$, each expectation value $\mathbb{E}\left(a_xb_y\right)$ contains only one nonzero term, the term in which $a_x=b_y=1$. These equalities are satisfied when Alice's i^{th} microscopic system and Bob's i^{th} microscopic system output 1s. Consequently, $\mathbb{E}\left(a_xb_y\right)$ equals the probability that $a_x=b_y=1$:

$$\mathbb{E}\left(a_{x}b_{y}\right) = \mathbb{P}\left(a_{x}=b_{y}=1\right). \tag{D1}$$

We calculate $\mathbb{E}(a_x b_y)$ when Alice and Bob follow the CHSH strategy outlined in App. C. The probability that Alice and Bob send responses 11, given questions xy, is

$$\mathbb{P}\left(a_x = b_y = 1\right) = \left|\left\langle --|R_z(\theta_x + \theta_y)|\Psi^-\right\rangle\right|^2. \tag{D2}$$

Since $ZZ|\Psi^{-}\rangle = -|\Psi^{-}\rangle$,

$$\left| \langle --|R_z(\theta_x + \theta_y)|\Psi^-\rangle \right|^2 = \left| \langle --|R_z(\theta_x + \theta_y)(ZZ)|\Psi^-\rangle \right|^2 \tag{D3}$$

$$= |\langle --| (ZZ) R_z(\theta_x + \theta_y) | \Psi^- \rangle|^2$$
 (D4)

$$= |\langle ++|R_z(\theta_x + \theta_y)|\Psi^-\rangle|^2. \tag{D5}$$

Hence the LHS of Eq. (D2) decomposes in terms of Eq. (D5) and the LHS of Eq. (D3):

$$\mathbb{P}(a_x = b_y = 1) = \frac{1}{2} \left[|\langle + + | R_z(\theta_x + \theta_y) | \Psi^- \rangle|^2 + |\langle - - | R_z(\theta_x + \theta_y) | \Psi^- \rangle|^2 \right]$$
 (D6)

$$= \frac{1}{2} P_{XX} (S_{\text{even}} | \Psi^{-}(\theta_x + \theta_y)). \tag{D7}$$

Substituting in from Eq. (C7) gives

$$\mathbb{P}(a_0 = b_0 = 1) = \frac{1}{2} P_{XX} (S_{\text{even}} | \Psi^-(3\pi/4))$$
(D8)

$$= \frac{1}{2}\sin^2(3\pi/8). \tag{D9}$$

Similarly, by Eq. (C8),

$$\mathbb{P}(a_1 = b_1 = 1) = \mathbb{P}(a_0 = b_1 = 1) = \frac{1}{2} P_{XX} (S_{\text{even}} | \Psi^-(3\pi/4))$$
(D10)

$$= \frac{1}{2}\sin^2(3\pi/8). \tag{D11}$$

Finally, Eq. (C11) implies that

$$\mathbb{P}(a_1 = b_1 = 1) = \frac{1}{2} P_{XX} (S_{\text{even}} | \Psi^-(9\pi/4))$$
(D12)

$$= \frac{1}{2}\sin^2(9\pi/8)$$
 (D13)

$$= \frac{1}{2} - \frac{1}{2}\sin^2(3\pi/8). \tag{D14}$$

Combining Equations (D9), (D11), and (D14) with Eq. (D1) yields

$$\mathbb{E}(a_0b_0) + \mathbb{E}(a_1b_0) + \mathbb{E}(a_0b_1) - \mathbb{E}(a_1b_1) = \mathbb{P}(a_0=b_0=1) + \mathbb{P}(a_1=b_0=1) + \mathbb{P}(a_0=b_1=1) - \mathbb{P}(a_1=b_1=1)$$
(D15)

$$= 2\sin^2(3\pi/8) - \frac{1}{2}. ag{D16}$$

D 2 Analysis of experimental error in quantum violation of the macroscopic Bell inequality

In the sketch of the proof of Theorem 2, we showed that [Eq. (19)]

$$\mathcal{B}(A_0', A_1', B_0', B_1') = 2\sqrt{2}. (D17)$$

The macroscopic random variables A'_0 , A'_1 , B'_0 , B'_1 were produced by noise-free measurements of perfectly prepared Bell states.

Noise can taint the setup, as discussed in Sec. I. To recap, we define

$$A_x = A_x' + r_{A_x}. (D18)$$

The random variable r_{A_x} represents noise whose variance is bounded: $\operatorname{Var}(r_{A_x}) \leq \epsilon N$. A_x represents the macroscopic outcome of a measurement made in the presence of noise. B_y and r_{B_y} are defined analogously.

In App. B, we showed that [Eq. (B7)]

$$|\mathcal{B}(A_0, A_1, B_0, B_1) - \mathcal{B}(A_0', A_1', B_0', B_1')| \le 16\epsilon - 32\sqrt{\epsilon}. \tag{D19}$$

Rearranging gives

$$\mathcal{B}(A_0, A_1, B_0, B_1) \ge \mathcal{B}(A_0', A_1', B_0', B_1') - 16\epsilon - 32\sqrt{\epsilon}. \tag{D20}$$

Substituting in from Eq. (D17) gives

$$\mathcal{B}(A_0, A_1, B_0, B_1) \ge 2\sqrt{2} - 16\epsilon - 32\sqrt{\epsilon},\tag{D21}$$

the desired result.

Appendix E EQUIVALENCE OF LOCAL QUANTUM CORRELATIONS AND GLOBAL CLASSICAL CORRELATIONS AS RESOURCES FOR VIOLATING THE MACROSCOPIC BELL INEQUALITY

We formalize the discussion in Sec. III with a theorem. To state the theorem cleanly and to avoid confusion with A_x and B_y , we introduce experimentalists Carol and Dan. Each has a system of N particles. Carol measures with settings x = 0, 1, and Dan measures with settings y = 0, 1. The macroscopic outcomes are the values of random variables C_x and D_y .

Like Alice and Bob, Carol and Dan obey assumption (a) in Sec. I. But Carol and Dan's systems can share global correlations, violating assumption (b). We assume that Carol and Dan's measurements suffer from no other errors.

Theorem 4. Carol and Dan can, with $2N \gg 1$ particles, produce correlations that satisfy

$$\mathcal{B}(C_0, C_1, D_0, D_1) = 2N. \tag{E1}$$

Proof. Carol and Dan can implement a probabilistic strategy, flipping an unbiased coin. If the coin falls heads-up, they fix their particles to output 1s, regardless of measurement settings. If the coin falls tails-up, all particles are fixed to output 0s. A straightforward calculation gives

$$Cov(C_0, D_0) = \frac{N^2}{2} - \left(\frac{N}{2}\right)^2 = \frac{N^2}{4}.$$
 (E2)

Similar calculations describe the other covariances, so

$$\mathcal{B}(C_0, C_1, D_0, D_1) = \frac{4}{N} \left(\frac{3N^2}{4} - \frac{N^2}{4} \right) = 2N.$$
 (E3)

Appendix F MACROSCOPIC CHSH GAME

We develop a macroscopic analog of the CHSH game, reviewed in App. C. Just as the CHSH game is built on the Bell-CHSH inequality, the macroscopic CHSH game is built on the macroscopic Bell inequality proven in Theorem 1. The macroscopic CHSH game differs from the microscopic CHSH game in three ways:

- 1. The macroscopic game is multiplayer. It involves 2N players, N Alices and N Bobs, who cannot communicate with each other. Each receives a question and responds. However, the verifier aggregates the Alices' responses and aggregates the Bobs' responses. We also place an important restriction on the players. We assume each Alice plays the game independently from all players except one Bob, and vice versa. This means each Alice can share randomness or entanglement with at most one Bob. The game's Alices play the same role as the microscopic particles in the main text. In the main text's photon-beam example, photons serve as the game's Alices and Bobs, and the beams serves as the game's aggregate Alice and aggregate Bob.
- 2. The game is multiround; several question-and-answer sessions take place. We assume the players lack memories, following the same strategy in every round.⁶ The verifier evaluates the players' performance after analyzing all the rounds' outcomes.
- 3. The verifier assigns to the players a score in [0, 1], rather than a win or a loss.

The rest of this appendix is organized as follows. We formulate the game in App. F 1. In App. F 2, we upper-bound the score achievable by players given only classical systems. We show how to violate the bound, using quantum systems, in App. F 3.

F 1 Definition of the macroscopic CHSH game

The macroscopic CHSH games is a multiround nonlocal game played with N memoryless Alices and N memoryless Bobs. In every round, the verifier randomly picks a question pair xy from the set $\{00, 01, 10, 11\}$. The question x is sent to every Alice, and the question y is sent to every Bob. Each Alice responds with one bit, as does each Bob. The verifier keeps a transcript of the questions and responses. After all the rounds, the verifier scores the game as follows:

- 1. The verifier calculates the average number \overline{A}_x of Alices who answer 1 to question x and the average number B_y of Bobs who answer 1 to question y, for all questions $x, y \in \{0, 1\}$.
- 2. The verifier assesses each round, using the following procedure. Label the round's questions x and y. Let A_x denote the number of Alices who reply 1 to x, and let B_y denote the number of Bobs who reply 1 to y. (A_x and B_y are values of random variables.) The verifier checks whether A_x and B_y satisfy two criteria, motivated below:
 - (a) If either number of 1s lies too close to the mean, the players lose the round: $|A_x \overline{A}_x| < \sqrt{N}$, or $|B_y \overline{B}_y| < \sqrt{N}$.
 - (b) Otherwise, the verifier checks whether

$$\operatorname{sgn}(\boldsymbol{A}_{\boldsymbol{x}} - \overline{A}_{x})\operatorname{sgn}(\boldsymbol{B}_{\boldsymbol{y}} - \overline{B}_{y}) = (-1)^{x \wedge y} \pmod{2}.$$
 (F1)

If this equation is true, the players win the round. If not, they lose.

3. The verifier assigns the players a score for the entire game: The verifier identifies the question pair $xy = x_0y_0$ on which the players won least frequently. The fraction of x_0y_0 rounds on which the players won becomes their score.

tiple trials. Multiple trials manifest, in the photon-beam example, as sequential measurements of Alice's beam's intensity and of Bob's beam's intensity. Alice's sequential measurements are measurements of independent sets of photons. The photons' independence is equivalent to the players' amnesia in the nonlocal game.

⁶ This requirement might seem strong from a nonlocal-games perspective. However, it is natural from the perspective of the macroscopic Bell test, presented in the main text, equivalent to our nonlocal game. We illustrate with the photon beams introduced in Sec. I. To perform the macroscopic Bell test, one evaluates the macroscopic Bell parameter (4) after running mul-

A few comments about this game are in order. First, we discuss the single-round win conditions, oppositely the order in which they are presented. Consider assigning the aggregated Alices a 1 if far more than the average number of constituent Alices respond with 1s and assigning the aggregated Alices a 0 if far fewer than the average number respond with 1s. Assign the aggregated Bobs a 1 or a 0 analogously. Condition 2b confirms that the aggregated Alices and aggregated Bobs satisfy the CHSH win condition (C1) in one round.

Condition 2a ensures that the players fail a round if their responses lie too close to the average responses. In the absence of this condition, the macroscopic CHSH game would reduce to the microscopic game: Imagine eliminating condition 2a and aggregating responses via $\operatorname{sgn}(A_x - \mathbb{A}_x)$ and $\operatorname{sgn}(B_y - \mathbb{B}_y)$. The players could follow a strategy according to which N-1 Alices (Bobs) responded deterministically. The final Alice's (Bob's) response would determine whether the number of 1s received were higher or lower than the average, determining the aggregate response. A microscopic response would control the macroscopic response.

 \sqrt{N} was chosen for the following reason. Each A_x and B_y is a sum of independent and identically distributed (i.i.d.) random variables. Consider the limit as $N \to \infty$. Consider the probability that A_x or B_y assumes a value $N^{1/2+\epsilon}$ away from its mean. This probability vanishes for all $\epsilon > 0$, by the central limit theorem. Hence fluctuations $\sim \sqrt{N}$ are the largest—most easily visible—fluctuations that can occur. The verifier must be able to detect these largest fluctuations and need not resolve finer fluctuations. A similar criterion is introduced in [35].

Second, we elucidate how the macroscopic Bell inequality's nonlinearity manifests in the macroscopic CHSH game. The inequality and the game distinguish classical randomness from pairwise entanglement (entanglement shared by each Alice with exactly one Bob and vice versa), without violating the principle of macroscopic locality [33–35]. The inequality succeeds by depending on probabilities nonlinearly (Sec. III). Therefore, also the game should involve nonlinearity. Each strategy specifies a set of four conditional probability density functions (PDFs), $\mathbb{P}(a,b \mid xy=00)$, $\mathbb{P}(a,b \mid xy=01)$, $\mathbb{P}(a,b \mid xy=10)$, and $\mathbb{P}(a,b \mid xy=11)$. The score is a function of the four PDFs and is nonlinear in each PDF. The reason is step 1: The verifier calculates average aggregate responses, then compares the actual aggregate responses with the averages.

This use of averages implies that the players should lack memories: Suppose that the players had only classical resources but had memories. The players could use different strategies in different rounds. Mixing strategies would change the averages, allowing players to win rounds that they would lose if they followed either strategy consistently.

F 2 Upper bound on the score achievable by classical players of the macroscopic CHSH game

We bound the classical players' score as follows. The random variables A_0 , A_1 , B_0 , and B_1 are distributed according to a multivariate Gaussian, by the central limit theorem. If these variables have limited variances and covariances, they are unlikely to satisfy the win criteria, (2a) and (2b). We prove this fact for $x \wedge y = 0$ in Lemma 3 and for $x \wedge y = 1$ in Corollary 1. The proofs consist of technical calculations regarding tails of multivariate Gaussians. Combining the lemma and corollary with Theorem 1 leads to Theorem 5: Every classical strategy has small covariance on at least on question pair. Hence the score achievable by classical players obeys an upper bound.

Lemma 3. Let \mathcal{X} and \mathcal{Y} denote random variables distributed according a multivariate Gaussian with variances $\sigma_{\mathcal{X}}^2 \leq N/4$ and $\sigma_{\mathcal{Y}}^2 \leq N/4$ and with covariance $Cov(\mathcal{X}, \mathcal{Y}) \leq N/7$. The probability that \mathcal{X} and \mathcal{Y} both far exceed their means is small:

$$\mathbb{P}\left(\mathcal{X} - \mathbb{E}\left(\mathcal{X}\right) \ge \sqrt{N} \wedge \mathcal{Y} - \mathbb{E}\left(\mathcal{Y}\right) \ge \sqrt{N}\right) \le 0.0051.$$
 (F2)

Proof. The proof is computational. For ease of notation, we shift \mathcal{X} and \mathcal{Y} so that each has mean 0. Let $\mathcal{Y}(x')$ denote the random variable \mathcal{Y} conditioned on the event $\mathcal{X} = x'$. We expand the probability in Eq. (F2):

$$\mathbb{P}\left(\mathcal{X} \ge \sqrt{N} \land \mathcal{Y} \ge \sqrt{N}\right) = \mathbb{P}\left(\mathcal{X} \ge \sqrt{N}\right) \mathbb{P}\left(\mathcal{Y} \ge \sqrt{N} \middle| \mathcal{X} \ge \sqrt{N}\right)$$
 (F3)

$$= \int_{\sqrt{N}}^{\infty} \mathbb{P}\left(\mathcal{X} = x'\right) \mathbb{P}\left(\mathcal{Y}(x') \ge \sqrt{N}\right) dx'. \tag{F4}$$

$$= \int_{\sqrt{N}}^{\infty} \int_{\sqrt{N}}^{\infty} \mathbb{P}(\mathcal{X} = x') \, \mathbb{P}(\mathcal{Y}(x') = y') dx' dy'. \tag{F5}$$

The theory of multivariate Gaussians implies that $\mathcal{Y}(x')$ is distributed according to a Gaussian with variance

$$\sigma_{\mathcal{Y}(x')} = \sqrt{\sigma_{\mathcal{Y}}^2 - \frac{\operatorname{Cov}(\mathcal{X}, \mathcal{Y})^2}{\sigma_{\mathcal{X}}^2}}$$
 (F6)

and mean

$$\mathbb{E}(\mathcal{Y}(x')) = \frac{x' \text{Cov}(\mathcal{X}, \mathcal{Y})}{\sigma_{\mathcal{X}}^2}.$$
 (F7)

We substitute the probabilities' Gaussian forms into Eq. (F5). If $\operatorname{erf}(z) := \frac{2}{\sqrt{\pi}} \int_0^z dt \ e^{-t^2}$ denotes the error function,

$$\mathbb{P}\left(\mathcal{X} \ge \sqrt{N} \land \mathcal{Y} \ge \sqrt{N}\right) = \int_{\sqrt{N}}^{\infty} \frac{1}{\sqrt{2\pi\sigma_{\mathcal{X}}^2}} \exp\left(-\frac{(x')^2}{2\sigma_{\mathcal{X}}^2}\right) \int_{\sqrt{N}}^{\infty} \frac{1}{\sqrt{2\pi\sigma_{\mathcal{Y}(x')}^2}} \exp\left(-\frac{[y' - \mathbb{E}(\mathcal{Y}(x'))]^2}{2\sigma_{\mathcal{Y}(x')}^2}\right) dy' dx' \qquad (F8)$$

$$= \int_{\sqrt{N}}^{\infty} \frac{1}{\sqrt{2\pi\sigma_{\mathcal{X}}^2}} \exp\left(-\frac{(x')^2}{2\sigma_{\mathcal{X}}^2}\right) \frac{1}{2} \left[1 - \operatorname{erf}\left(\frac{\sqrt{N} - \mathbb{E}(\mathcal{Y}(x'))}{\sqrt{2}\sigma_{\mathcal{Y}(x')}}\right)\right] dx'$$
 (F9)

$$= \int_{1}^{\infty} \frac{1}{\sqrt{2\pi\sigma_{\mathcal{X}}^{2}/N}} \exp\left(-\frac{(x')^{2}}{2\sigma_{\mathcal{X}}^{2}/N}\right) \frac{1}{2} \left[1 - \operatorname{erf}\left(\frac{1 - \mathbb{E}(\mathcal{Y}(x'))}{\sqrt{2}\sigma_{\mathcal{Y}(x')}/\sqrt{N}}\right)\right] dx'.$$
 (F10)

By assumption, $\sigma_{\mathcal{X}} \leq \sqrt{N}/2$, $\sigma_{\mathcal{Y}} \leq \sqrt{N}/2$, and $\operatorname{Cov}(\mathcal{X}, \mathcal{Y}) \leq \sqrt{N/7}$. By the Cauchy-Schwarz inequality, $\sqrt{\sigma_{\mathcal{X}}^2 \sigma_{\mathcal{Y}}^2} \geq \operatorname{Cov}(\mathcal{X}, \mathcal{Y})$ [Ineq. (B3)]. We numerically optimize the probability (F10) subject to these constraints [67]. The probability maximizes when $\sigma_{\mathcal{X}}$, $\sigma_{\mathcal{Y}}$, and $\operatorname{Cov}(\mathcal{X}, \mathcal{Y})$ assume their maximum possible values: $\sigma_{\mathcal{X}} = \sigma_{\mathcal{Y}} = \sqrt{N}/2$, and $\operatorname{Cov}(\mathcal{X}, \mathcal{Y}) = N/7$. The maximum probability lies slightly below 0.0051.

Corollary 1. Let \mathcal{X} and \mathcal{Y} denote random variables distributed according to a multivariate Gaussian with variances $\sigma_{\mathcal{X}}^2 \leq N/4$ and $\sigma_{\mathcal{Y}}^2 \leq N/4$ and with covariance $Cov(\mathcal{X}, \mathcal{Y}) \leq -N/7$. The probability that \mathcal{X} far exceeds its mean while \mathcal{Y} lies far below its mean is small:

$$\mathbb{P}\left(\mathcal{X} - \mathbb{E}\left(\mathcal{X}\right) \ge \sqrt{N} \wedge \mathcal{Y} - \mathbb{E}\left(\mathcal{Y}\right) \le -\sqrt{N}\right) \le 0.0051. \tag{F11}$$

Proof. Apply Lemma 3 to the random variables \mathcal{X} and $-\mathcal{Y}$.

Theorem 5. Classical players can achieve an average score of at most 0.0102 in the macroscopic CHSH game, if the number 2N of players is sufficiently large.

Proof. By the multivariate central limit theorem, the random variables A_0 , A_1 , B_0 , and B_1 come to obey multivariate Gaussian distributions in the large-N limit. Let xy denote an arbitrary question pair. If $x \wedge y = 0$, the players can win in two ways: (i) The number A_x of Alices who respond 1 lies far above the mean number \overline{A}_x who respond 1. Meanwhile, the number B_y of Bobs who respond 1 lies far above the mean number \overline{B}_y . That is,

$$A_x - \overline{A}_x \ge \sqrt{N} \wedge B_y - \overline{B}_y \ge \sqrt{N}.$$
 (F12)

(ii) A_x lies far below its average, while B_y lies far below its average:

$$A_x - \overline{A}_x \le -\sqrt{N} \wedge B_y - \overline{B}_y \le -\sqrt{N}.$$
 (F13)

The players' probability of winning via (i) was bounded in Lemma 3. Their probability of winning via (ii) is the same, by the multivariate Gaussian's symmetry. Hence the players' total probability of winning on $xy : x \land y = 0$ is

$$\mathbb{P}\left(A_{x} - \mathbb{E}\left(A_{x}\right) \geq \sqrt{N} \wedge B_{y} - \mathbb{E}\left(B_{y}\right) \geq \sqrt{N}\right) + \mathbb{P}\left(A_{x} - \mathbb{E}\left(A_{x}\right) \leq -\sqrt{N} \wedge B_{y} - \mathbb{E}\left(B_{y}\right) \leq -\sqrt{N}\right)$$
(F14)

$$=2\mathbb{P}\left(A_{x}-\mathbb{E}\left(A_{x}\right)\geq\sqrt{N}\wedge B_{y}-\mathbb{E}\left(B_{y}\right)\geq\sqrt{N}\right).\tag{F15}$$

The second line follows from the multivariate Gaussian's symmetry.

Now, suppose that $x \wedge y = 1$. The players win if the number A_x of Alices who reply 1 lies far above/below its mean while the number B_y of Bobs who reply 1 lies far below/above its mean:

$$A_x - \overline{A}_x \ge \sqrt{N} \wedge B_y - \overline{B}_y \le -\sqrt{N}$$
, or (F16)

$$A_x - \overline{A}_x \le -\sqrt{N} \wedge B_y - \overline{B}_y \ge \sqrt{N}$$
 (F17)

These two events have equal probabilities of occurring. Hence the players have a win probability of

$$2\mathbb{P}\left(A_{x} - \mathbb{E}\left(A_{x}\right) \ge \sqrt{N} \wedge B_{y} - \mathbb{E}\left(B_{y}\right) \le -\sqrt{N}\right). \tag{F18}$$

We now invoke the macroscopic Bell inequality. For simplicity, we have not defined noise or classical global correlations in the game. We therefore set $\epsilon = 0$ in Theorem 1. The theorem, with the definition (4), implies that

$$Cov(A_0, B_0) + Cov(A_0, B_1) + Cov(A_1, B_0) - Cov(A_1, B_1) \le 4N/7.$$
 (F19)

A minimimax argument gives

$$\min \left\{ \text{Cov} (A_0, B_0), \text{Cov} (A_0, B_1), \text{Cov} (A_1, B_0), -\text{Cov} (A_1, B_1) \right\} \le N/7.$$
 (F20)

Therefore, some question pair xy satisfies either $x \wedge y = 0$ and $Cov(A_x, B_y) \leq N/7$ or $x \wedge y = 1$ and $Cov(A_x, B_y) \geq -N/7$. Furthermore, each A_x and each B_y is a sum of N independent random variables, each of which has a variance of $\leq 1/4$. Hence

$$Var(A_0), Var(A_1), Var(B_0), Var(B_1) \le N/4.$$
 (F21)

Consider the (A_x, B_y) that achieves the minimization in Ineq. (F20). It satisfies the assumptions in Lemma 3 and Corollary 1. By the lemma and Eq. (F15), and by the corollary and Eq. (F18), this (A_x, B_y) satisfies the win conditions with probability $\leq 2 \times 0.0051 = 0.0102$. The score equals the minimum, over all xy pairs, of the probability that the players win on xy. Hence the score ≤ 0.0102 , as claimed.

F 3 Superclassical score in the macroscopic CHSH game

We have upper-bounded the score achievable by classical players of the macroscopic CHSH game. Now, we show that players can violate this bound, given quantum resources. The proof is constructive; we exhibit a superclassical strategy. It is built on the strategy shown, in App. C, to win the microscopic CHSH game with a superclassical probability.

Theorem 6. Players given quantum resources can achieve a score of ≥ 0.0150 in the macroscopic CHSH game.

Proof. As in the proof of Theorem 2, each Alice-Bob pair adopts the conventional CHSH strategy (App. C): Each pair shares a singlet. When Alice measures any observable, she has a probability 1/2 of obtaining +1, and responding 1 to the verifier, and a probability 1/2 of obtaining -1, and responding 0. The same is true of Bob. Hence the aggregated Alice responses and the aggregated Bob responses obey

$$\mathbb{E}(A_0) = \mathbb{E}(A_1) = \mathbb{E}(B_0) = \mathbb{E}(B_1) = N/2 \tag{F22}$$

and

$$Var(A_0) = Var(A_1) = Var(B_0) = Var(B_1) = N/4.$$
 (F23)

According to Equations (7), (D1), (D9), (D11), and (D14), A_0 , A_1 , B_0 , and B_1 satisfy also

$$Cov(A_0, B_0) = Cov(A_0, B_1) = Cov(A_1, B_0) = -Cov(A_1, B_1)$$
 (F24)

$$= \sum_{i=1}^{N} \text{Cov}\left(a_0^{(i)}, b_0^{(i)}\right)$$
 (F25)

$$= \sum_{i=1}^{N} \left[\mathbb{E} \left(a_0^{(i)} \right) \mathbb{E} \left(b_0^{(i)} \right) \right]$$
 (F26)

$$= \sum_{i=1}^{N} \left[\mathbb{P}\left(a_0^{(i)} = b_0^{(i)} = 1 \right) - \frac{1}{2} \cdot \frac{1}{2} \right]$$
 (F27)

$$= N\left[\frac{1}{2}\sin^2\left(\frac{3\pi}{8}\right) - \frac{1}{4}\right] \tag{F28}$$

$$= N/(4\sqrt{2}). \tag{F29}$$

We can numerically bound the mean score averaged over instances of the (multiround) game. The computation bounding the mean win probability on the question pair 00 is given here. The other calculations are similar and produce identical results.

By the multivariate central limit theorem, the joint distribution over the random variables A_0 and B_0 is a multivariate Gaussian with means N/2 and covariance matrix

$$\Sigma = \begin{pmatrix} \frac{N}{4} & \frac{N}{4\sqrt{2}} \\ \frac{N}{4\sqrt{2}} & \frac{N}{4} \end{pmatrix}. \tag{F30}$$

The players win if A_0 and B_0 both lie above or both lie below their means by at least \sqrt{N} . This event occurs with probability

$$\mathbb{P}\left(A_0 \ge N/2 + \sqrt{N} \ \land \ B_0 \ge N/2 + \sqrt{N}\right) + \mathbb{P}\left(A_0 \le N/2 - \sqrt{N} \ \land \ B_0 \le N/2 - \sqrt{N}\right) \ge 0.0150. \tag{F31}$$

The bound was computed numerically [67].

Appendix G TOY APPLICATION TO POSNER MOLECULES

In Sec. III, we introduced a potential application of the macroscopic Bell inequality to Posner molecules. Posners are beginning to be characterized experimentally. If they are found to retain coherences, entanglement should be tested for [39]. How can it be, since the operations conjectured to be performable on Posners differ from the operations used in conventional Bell tests [38]? We begin answering that question here, though further work is needed. We construct a partially macroscopic Bell test implementable with the operations conjectured to be performable on Posners [36, 38]. The test relies on macroscopic intensity measurements but microscopic manipulations of Posners.

The background needed to understand this appendix can be found in the following places. First, information about Posners appears in [38], particularly in Sections 2.1, 3.1, 3.2, 3.4, and 3.7. Second, useful background appears in this paper's Sec. III, App. C, and App. G 1. Third, calculations involving Posner states were performed with code that was originally written by E. Crosson for [38] and was repurposed with her permission [67].

The rest of this appendix is structured as follows. The first two sections offer a warmup: Appendix G 1 overviews the tools used. Appendix G 2 introduces a strategy for winning the CHSH game with a superclassical probability, using a finely controlled system of a few Posners. We sketch a many-Posner Bell test in App. G 3. In App. G 4, we analyze the sketch, identify its shortcomings, and discuss opportunities for sharpening it.

G 1 Preliminaries needed for the Posner Bell test

In Sec. G 1 i, we discuss the operations needed to perform our Posner Bell test. In Sec. G 1 ii, we introduce four facts that underlie the analysis of the Posner Bell test.

G 1 i Operations needed to implement the Posner Bell test

These operations can be performed in principle, if Fisher conjectures correctly about Posner biochemistry [36]. That is, these operations can be implemented within the Posner model of quantum computation, or with *Posner operations*, defined in Sec. 3.4 of [38]. However, some operations require impractical microscopic control.

- 1. Preparation of singlets of phosphate nuclear spins: We assume that phosphates' phosphorus nuclear spins can be prepared in the singlet state, $|\Psi^{-}\rangle = \frac{1}{\sqrt{2}} (|01\rangle |10\rangle)$ (see Sections 2.1 and 3.4 of [38]). Such a singlet has been conjectured to form when the enzyme pyrophosphatase hydrolyzes a diphosphate into two phosphates [36, 37].
- 2. Controlled Posner formation: We assume that Posners can be formed with phosphates laid out in arbitrary arrangements, subject to the restrictions of the Posner's geometry (see Sections 3.1.2–3.1.4, 3.4, and 3.7 of [38]). This assumption may seem unreasonable. We can mitigate the unreasonableness slightly, because the assumption is required only for setting up the Posner Bell test. The ability to detect and postselect on Posners in desired geometries would suffice.

In particular, we assume the ability to create two Posners that share six singlets in a geometrically symmetric arrangement. This "six singlets shared" state is presented in Sec. 3.7 of [38] and reproduced here in Fig. 1. We denote this state by $|\psi_{AB}^{\text{ent}}\rangle$, wherein A and B label the Posners.

3. τ rotations: A Posner has a sixfold rotational symmetry. Consider the operator that represents a rotation about the symmetry axis. The operator has eigenvalues $\tau = 0, \pm 1$. The Posner Bell test requires the ability to map some states of a Posner to another τ sector. Such a rotation can be accomplished via multiple mathematical operations, we found via direct calculation [67]. One operation is a rotation of one of the Posner's qubits with the Pauli z-operator, σ_z . We focus on this implementation for concreteness.

We assume the existence of an operator $\mathcal{R}_z(\theta)$ that represents the desired rotation. For specificity, we assume that the rotated qubit is the qubit labeled 1 in [38] (see Fig. 1 in the present paper). When we need to distinguish between Posners, we use the notation $\mathcal{R}_z(\theta)_A$ to denote the operator $\mathcal{R}_z(\theta)$ applied to Posner A.

 $\mathcal{R}_z(\theta)$ can be effected physically, e.g., as described in Sections 3.4 and 3.8 of [38]: Let phosphate 1 form a Posner A with other phosphates and with calcium ions. Applying a magnetic field to A will rotate all six qubits, with $[R_z(\theta)]^{\otimes 6}$. If the pH rises, Posner A will likely hydrolyze, or break apart. The pH can then be lowered. Phosphate 1 can find new phosphates with which to form a Posner B. Posner B will have undergone $\mathcal{R}_z(\theta)_B$. Other means of effecting $\mathcal{R}_z(\theta)$ may be possible.

4. Posner-binding measurement: Suppose that Posners A and B approach each other such that their symmetry axes are parallel and point oppositely each other. We call this arrangement the prebinding orientation, following [38]. Quantum-chemistry calculations suggest that the Posners can bind together [55]. This measurement projects Posners A and B into the subspace labeled by $\tau_A + \tau_B = 0$ (if the Posners bind) or onto the orthogonal subspace (if the Posners do not). Following [38], we denote by Π_{AB} the projector onto the Posner-binding subspace.

We assume that an experimentalist can observe the number of such bindings. A method is proposed in [39]: Calcium indicators are added to the Posner-containing test tube. Bound-together Posners would move slowly, becoming susceptible to attack by hydrogen ions H^+ and magnesium ions Mg^{2+} . These ions could outcompete the positively charged calcium ions Ca^{2+} in binding to the negatively charged phosphate ions PO_4^{3-} . The invaders would hydrolyze the Posners, breaking the molecules into their constituent ions. The calcium indicators would bind to the calcium ions Ca^{2+} , then fluoresce. An experimentalist could detect the fluorescence.

Our proposal sharpens the inspirational sketch, in [39], of a test for entanglement between Posners. There, Posners in different test tubes were imagined to share entanglement. Posners in each test tube would bind, and each test tube would fluoresce. The intensities of the test tubes' fluorescence were imagined to exhibit correlations. We add that, to infer that Posners shared entanglement, one must observe not just any correlations between the intensities. Some correlations produceable with entanglement can be recapitulated with classical resources. We begin constructing a means of observing nonclassical correlations, using the macroscopic Bell inequality (Theorem 1).

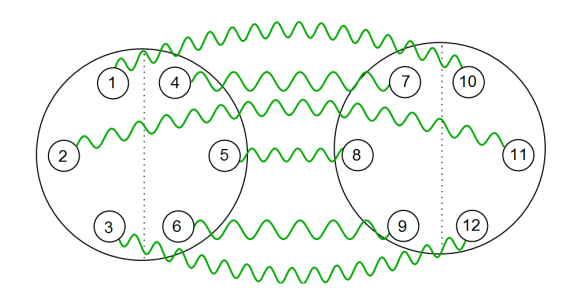


FIG. 1: Symmetric "six singlets shared" configuration of two Posner molecules: Reprinted from [38], with permission from Elsevier.

First, all the phosphorus nuclear spins in the state $|\psi_{AB}^{\text{ent}}\rangle$ are in copies of $|\Psi^{-}\rangle$. Each phosphate in Posner A is entangled with the phosphate at the corresponding position in Posner B. As shown in App. C,

$$[R_z(\theta_1) \otimes R_z(-\theta_2)]|\Psi^-\rangle = [R_z(\theta_1 + \theta_2) \otimes \mathbb{1}]|\Psi^-\rangle. \tag{G1}$$

The Posner analog (operation 3 in App. G 1 i) has the form

$$[\mathcal{R}_z(\theta_1)_A \otimes \mathcal{R}_z(-\theta_2)_B]|\psi_{AB}^{\text{ent}}\rangle = \mathcal{R}_z(\theta_1 + \theta_2)_A|\psi_{AB}^{\text{ent}}\rangle. \tag{G2}$$

Second, $|\psi_{AB}^{\rm ent}\rangle$ is a superposition of states in which the Posners' τ values sum to zero. This fact was first pointed out in [38]: Consider Posners that occupy the state $|\Psi_{AB}^{\rm ent}\rangle$ and the prebinding orientation. The Posners were observed to have a unit probability of binding (under the assumptions of Fisher's model).

Third, suppose that Posners A and B occupy the state $|\psi_{AB}^{\text{ent}}\rangle$, while Posners A' and B' occupy the state $|\psi_{A'B'}^{\text{ent}}\rangle$. Suppose that A assumes the prebinding orientation with A' and that B assumes the prebinding orientation with B'. A pair's binding is represented with a 1. The two pairs' bits have even parity in two cases, if both pairs bind or both pairs fail to bind. If the bits have even parity, the four-Posner state is projected with

$$\Pi_{\text{even}} = \Pi_{AA'}\Pi_{BB'} + (\mathbb{1} - \Pi_{AA'})(\mathbb{1} - \Pi_{BB'}). \tag{G3}$$

The binding-measurement outcomes have even parity, we claim:

$$|\Pi_{\text{even}}|\psi_{AB}^{\text{ent}}\rangle|\psi_{A'B'}^{\text{ent}}\rangle|^2 = 1. \tag{G4}$$

Either both pairs bind or both fail to bind. Equation (G4) can be checked computationally [67] and with the following logic: In $|\psi_{AB}^{\text{ent}}\rangle$, $\tau_A + \tau_B = 0$. In $|\psi_{A'B'}^{\text{ent}}\rangle$, $\tau_{A'} + \tau_{B'} = 0$. Hence $\tau_{\text{total}} = \tau_A + \tau_{A'} + \tau_B + \tau_{B'} = 0$. In contrast, any state in the image of the projector $\mathbb{1} - \Pi_{\text{even}} = \Pi_{AA'}(\mathbb{1} - \Pi_{BB'}) + (\mathbb{1} - \Pi_{AA'})\Pi_{BB'}$ has a $\tau_{\text{total}} \neq 0$.

Fourth, we continue to consider the four-Posner state $|\psi_{AB}^{\text{ent}}\rangle|\psi_{A'B'}^{\text{ent}}\rangle$. Consider rotating a qubit with $\mathcal{R}_z(\theta_1)_A$. The state of Posners A and B is rotated out of the $\tau_A + \tau_B = 0$ sector. This claim can be checked via direct calculation [67]. The even-parity-binding probability, $|\Pi_{\text{even}}\mathcal{R}_z(\theta_1)_A|\psi_{AB}^{\text{ent}}\rangle|\psi_{A'B'}^{\text{ent}}\rangle|^2$, decreases as the rotation angle θ_1 grows. We solve for this relationship numerically [67] and present the results in Fig. 2.

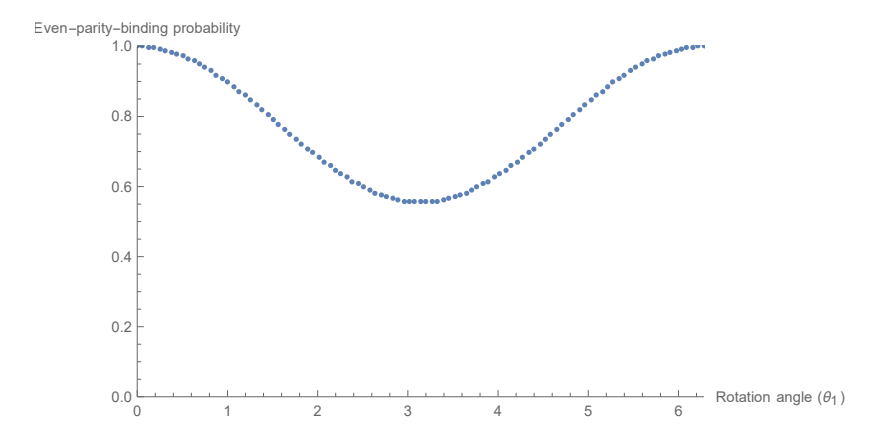


FIG. 2: Probability of even-parity binding vs. rotation angle: Probability $\left|\Pi_{\text{even}}\mathcal{R}_z(\theta_1)_A|\psi_{A'B'}^{\text{ent}}\rangle\right|^2$ that Posner A binds to Posner A' while B binds to B', after a qubit in A is rotated through an angle θ_1 .

G 2 Nonlocal game for a system of few Posners

We define the game in Sec. G 2 i. The game is adapted from the original CHSH game (App. C): As in the original game, the Posner game's players use singlets and rotations. But Posner-holding players cannot measure $\sigma_x \otimes \sigma_x$. So they share 12 singlets, rather than one, and perform Posner-binding measurements, rather than measuring Pauli operators. Section G 2 ii shows that Posners can win the game with a superclassical probability, in principle, if Fisher's model is correct. This result is not obvious: The quantum operations undergone by Posners in Fisher's model are nonstandard and might not contain a universal gate set [38]. Our proof rests, however, on fine control over the operations conjectured to be implementable.

We consider two experimentalists, Alice and Bob. Each can perform the operations described in App. G 1. Before the test begins, the players prepare two copies of the two Posner-state $|\psi^{\text{ent}}\rangle$. Posner A shares entanglement with Posner B, and A' shares entanglement with B'. Alice takes A and A', while Bob takes B and B'. Alice and Bob separate, and each experimentalist receives a question from a verifier. The experimentalists aim to produce responses that win the CHSH game (App. C) with a superclassical probability.

Alice and Bob's procedures are almost identical, but we describe Alice's approach first. If Alice receives the question 0, she rotates Posner A with $\mathcal{R}_z(-\pi/8)_A$. If she receives a 1, she rotates with $\mathcal{R}_z(3\pi/8)_A$. Afterward, she performs the Posner-binding measurement between Posners A and A'. If the Posners bind, she sends the verifier a 1. If the Posners fail to bind, she sends a 0.

Bob's procedure is similar. However, he rotates Posner B with $\mathcal{R}_z(\pi/8)_B$, given the question y = 0, and rotates with $\mathcal{R}_z(-3\pi/8)_B$, given y = 1. His binding measurement is on Posners B and B'.

G 2 ii Analysis of the Bell test for a few Posners

If Posners share entanglement, we now show, they can outperform classical resources in the CHSH game, in principle, under Fisher's assumptions.

Claim 1. Alice and Bob can win the nonlocal game for a few Posners with a superclassical probability of $\geq 79.5\%$, given fine control over the operations implementable in principle in Fisher's model.

Proof. Assume that Alice rotates Posner A with an angle θ_1 , while Bob rotates B with an angle θ_2 . By the test's construction, the experimentalists' probability of sending the verifier an even-parity response pair is

$$|\Pi_{\text{even}} \left[\mathcal{R}_z(\theta_1)_A \otimes \mathcal{R}_z(\theta_2)_B \right] |\psi_{AB}^{\text{ent}}\rangle |\psi_{A'B'}^{\text{ent}}\rangle |^2 = |\Pi_{\text{even}} \left[\mathcal{R}_z(\theta_1 - \theta_2)_A \right] |\psi_{AB}^{\text{ent}}\rangle |\psi_{A'B'}^{\text{ent}}\rangle |^2.$$
 (G5)

The equality follows from Eq. (G2). We evaluate this probability for all possible question pairs in Table II [67].

Questions	$\theta_1 - \theta_2$	Even-parity-response probability
00	$-\pi/4$	0.934
01	$\pi/4$	0.934
10	$\pi/4$	0.934
11	$3\pi/4$	0.620

TABLE II: The probability that players provide an even-parity response pair ab to the possible question pair xy in the few-Posner CHSH game. The first bit in the "questions" column labels the question x sent to Alice. The second bit labels the question y sent to Bob.

In each round of the CHSH game, the verifier selects the question pair uniformly randomly. The winning response pairs for the question pairs 00, 01, and 10 have even parity. The winning response pair for the question pair 11 has odd parity. Therefore, the overall win probability for the few-Posner game is

$$\frac{3}{4} \times 0.934 + \frac{1}{4} \times (1 - 0.620) > 0.795. \tag{G6}$$

The angles used by Alice and Bob (Sec. G 2 i) differ from the angles used in the conventional CHSH game (App. C). The reason is, in the conventional game, Alice and Bob share a singlet, $|\Psi^-\rangle := \frac{1}{\sqrt{2}}(|01\rangle - |10\rangle)$. In the Posner game, Alice and Bob share entangled a pair of Posners. For the game's purposes, the Posners' τ degrees of freedom resemble qubits in the maximally entangled state $|\Phi^+\rangle := \frac{1}{\sqrt{2}}(|00\rangle + |11\rangle)$. If Alice and Bob shared a copy of $|\Phi^+\rangle$ in the conventional CHSH game, they would use the rotations in App. G 2 i. This small-scale Posner Bell test informs our macroscopic Posner Bell test, introduced next.

G 3 Sketch of macroscopic Posner Bell test

We envision a three-dimensional tank of aqueous fluid. A glass plate coincides with the xy-plane. Along the x-axis is a slit in which pyrophosphatase enzymes are lodged. Diphosphate ions are poured above the xy-plane and waft downward on currents propelled from above.

The diphosphates can traverse the plane only through the enzymes. Suppose that an enzyme hydrolyzes a diphosphate, breaking the diphosphate into two phosphates (PO_4^{3-}). The phosphorus (^{31}P) nuclear spins form a singlet, $\frac{1}{\sqrt{2}}(|\uparrow\downarrow\rangle - |\downarrow\uparrow\rangle)$, according to the dynamical selection rule posited by Fisher and Radzihovsky [36, 37]. We assume that, during the hydrolyzation and release, the enzyme changes shape, such that the diphosphate can enter the fluid below the xy-plane.

Below the xy-plane, two currents sweep fluid away from the x-axis. One current sweeps toward the +y-axis, where Alice collects the fluid. The other current sweeps toward the -y-axis, where Bob collects the fluid. Alice and Bob share singlets. Alice and Bob add calcium ions, Ca^{2+} , to their fluids. Posners form. Each players divides his/her fluid among 3 test tubes. Alice holds test tubes A_1 , A_2 , and A_3 . Bob holds test tubes B_1 , B_2 , and B_3 .

A verifier sends a question x=0,1 to Alice and a question y=0,1 to Bob (App. F). Alice and Bob agreed, before collecting the Posners, to follow the strategy for winning the few-Posner Bell test with a superclassical probability (App. G 2): Upon receiving x=0, Alice applies a magnetic field to test tube 1. The field implements the rotation $R_z(-\pi/8)$ on all the Posners in the test tube. If Alice receives x=1, she applies a field that implements $R_z(3\pi/8)$. Bob's strategy is similar but involves opposite signs: Given y=0, he applies a magnetic field that implements $R_z(\pi/8)$ on all the qubits in his 1 test tube. Given y=1, he applies $R_z(-3\pi/8)$.

Each player lowers the pH in test tubes 1 and 2. The H^+ ions outcompete positively charged Ca^{2+} ions in binding to the negatively charge phosphorus ions (PO_4^{3-}) . The protons hydrolyze the Posners. Each player mixes his/her 1 and 2 test tubes, then raises the pH. New Posners form. Some Posners contain phosphorus nuclei whose spins are rotated relative to the spins of the Posner's other phosphorus nuclei.

Each player mixes his/her combined 1 and 2 test tubes with test tube 3, whose qubits have not been rotated. Then, each player adds calcium indicators to the test tube and lowers the pH. Posners are hoped to approach each other in the prebinding orientation. In Fisher's model, some fraction of these Posners will bind. The fraction depends on the entanglement and on the binding of Posners in the other player's test tube. The bound-together Posners move slowly, forming easy targets for H⁺ ions. The ions hydrolyze the bound-together Posners, flooding the test tubes with calcium. The calcium binds to the calcium indicators, which fluoresce.

Alice and Bob measure the fluorescence's intensity. After completing many trials, they compute the covariances between their intensities, then estimate the macroscopic Bell parameter [Eq. (4)]. A superclassical value (Sec. 1) certifies entanglement between Posners, if the experiment satisfies the assumptions in Sec. I. The experiment sketched here likely does not satisfy the assumptions. We delineate reasons, and opportunities for improving the sketch, in the next section.

G 4 Analysis of sketch of Posner Bell test

Much work remains to be done to shore up the Posner Bell test theoretically and to ensure its experimental feasibility. First, the macroscopic Bell inequality needs extending. Theorem 1 relies on each particle's interacting with, at most, one other particle. Each Posner can share entanglement with up to six other Posners. The extension from one to six requires a change to the inequality but maintains interactions' locality.

Second, much could go awry during an implementation of the protocol in Sec. G 3. A not-necessarily-complete list of loopholes include the following: (i) Enzymes might release separated phosphates into the fluid above the glass plane. (ii) A current could sweep two entangled-together phosphates toward the same test tube. (iii) The phosphates will assume random locations in the Posners. The "six singlets shared" states (Fig. 1) might form rarely. (iv) The entangled phosphates spend time outside the Posners conjectured to protect coherence. The phosphorus nuclear spins might decohere before Alice and Bob can complete their trial. Time scales must be estimated and compared, as in Section 3.8 and App. K of [38]. (v) Posners in the same test tube might have a low probability of assuming the prebinding orientation. The overall binding rate might therefore be too low. (vi) H⁺ ions can hydrolyze not only bound-together Posners, but also individual Posners. Individual Posners' hydrolyzation will add noise to the intensity measurements.

REFERENCES

- [2] A. J. Leggett, Journal of Physics: Condensed Matter 14, R415 (2002).
- [3] M. Blencowe, Science 304, 56 (2004), https://science.sciencemag.org/content/304/5667/56.full.pdf.
- [4] S. Gerlich et al., Nature Communications 2, 263 (2011).
- [5] E. E. Wollman et al., Science 349, 952 (2015), https://science.sciencemag.org/content/349/6251/952.full.pdf.
- [6] R. Kaltenbaek et al., EPJ Quantum Technology 3, 5 (2016).
- [7] P. Yao and S. Hughes, Opt. Express 17, 11505 (2009).
- [8] I. Marinković et al., Phys. Rev. Lett. 121, 220404 (2018).
- [9] R. Schmied et al., Science 352, 441 (2016), https://science.sciencemag.org/content/352/6284/441.full.pdf.
- [10] M. D. Reid, W. J. Munro, and F. De Martini, Phys. Rev. A 66, 033801 (2002).
- [11] N. D. Mermin, Phys. Rev. D 22, 356 (1980).
- [12] P. D. Drummond, Phys. Rev. Lett. 50, 1407 (1983).
- [13] N. D. Mermin, Phys. Rev. Lett. 65, 1838 (1990).
- [14] M. Ardehali, Phys. Rev. A 46, 5375 (1992).
- [15] A. V. Belinskiĭ and D. N. Klyshko, Physics-Uspekhi 36, 653 (1993).
- [16] D. Collins, N. Gisin, N. Linden, S. Massar, and S. Popescu, Phys. Rev. Lett. 88, 040404 (2002).
- [17] E. G. Cavalcanti, C. J. Foster, M. D. Reid, and P. D. Drummond, Phys. Rev. Lett. 99, 210405 (2007).
- [18] Q. Y. He, E. G. Cavalcanti, M. D. Reid, and P. D. Drummond, Phys. Rev. A 81, 062106 (2010).
- [19] Q. Y. He, P. D. Drummond, and M. D. Reid, Phys. Rev. A 83, 032120 (2011).
- [20] N. J. Engelsen, R. Krishnakumar, O. Hosten, and M. A. Kasevich, Phys. Rev. Lett. 118, 140401 (2017).
- [21] B. J. Dalton, (2018), 1812.09651.
- [22] J. Tura et al., Science 344, 1256 (2014), https://science.sciencemag.org/content/344/6189/1256.full.pdf.
- [23] J. Tura et al., Annals of Physics **362**, 370 (2015).
- [24] M. Stobińska, P. Sekatski, A. Buraczewski, N. Gisin, and G. Leuchs, Phys. Rev. A 84, 034104 (2011).
- [25] M. Żukowski and i. c. v. Brukner, Phys. Rev. Lett. 88, 210401 (2002).
- [26] B. J. Dalton, Euro. Phys. J. Special Topics **227**, 20692083 (2019).
- [27] M. D. Reid, Q.-Y. He, and P. D. Drummond, Frontiers of Physics 7, 72 (2012).
- [28] S. Barz, G. Cronenberg, A. Zeilinger, and P. Walther, Nature Photonics 4, 553 (2010).
- [29] H. Bernien et al., Nature 497, 86 (2013).
- [30] J. Laurat, K. S. Choi, H. Deng, C. W. Chou, and H. J. Kimble, Phys. Rev. Lett. 99, 180504 (2007).
- [31] J. Hofmann et al., Science 337, 72 (2012), https://science.sciencemag.org/content/337/6090/72.full.pdf.
- [32] B. Casabone et al., Phys. Rev. Lett. 111, 100505 (2013).
- [33] M. Navascus and H. Wunderlich, Proceedings of the Royal Society A: Mathematical, Physical and Engineering Sciences 466, 881 (2010), https://royalsocietypublishing.org/doi/pdf/10.1098/rspa.2009.0453.
- [34] T. H. Yang, M. Navascués, L. Sheridan, and V. Scarani, Phys. Rev. A 83, 022105 (2011).
- [35] M. Navascués, Macroscopic Locality (Springer, Netherlands, 2016), pp. 439–463.
- [36] M. P. A. Fisher, Annals of Physics **362**, 593 (2015).
- [37] M. P. A. Fisher and L. Radzihovsky, Proceedings of the National Academy of Sciences 115, E4551 (2018), https://www.pnas.org/content/115/20/E4551.full.pdf.
- [38] N. Yunger Halpern and E. Crosson, Annals of Physics 407, 92 (2019).
- [39] M. P. A. Fisher, International Journal of Modern Physics B **31**, 1743001 (2017), http://www.worldscientific.com/doi/pdf/10.1142/S0217979217430019.
- [40] Z. Fifer et al., Phys. Rev. E 99, 031101(R) (2019).
- [41] V. Pozsgay, F. Hirsch, C. Branciard, and N. Brunner, Phys. Rev. A 96, 062128 (2017).
- [42] P. G. Kwiat et al., Physical Review Letters 75, 4337 (1995).
- [43] J. F. Clauser, M. A. Horne, A. Shimony, and R. A. Holt, Phys. Rev. Lett. 23, 880 (1969).
- [44] H. Buhrman, R. Cleve, J. Watrous, and R. de Wolf, Phys. Rev. Lett. 87, 167902 (2001), quant-ph/0102001.
- [45] M. Reid, arXiv preprint quant-ph/0101052 (2001).
- [46] M. Reid, New tests of macroscopic local realism, in Directions in Quantum Optics, pp. 176–186, Springer, 2001.
- [47] R. Cleve, P. Høyer, B. Toner, and J. Watrous, Consequences and limits of nonlocal strategies, in Proc. 19th Annual IEEE Conf. Computational Complexity, pp. 236–249, 2004, quant-ph/0404076.
- [48] J. Preskill, Lecture notes for ph219/cs219: Quantum information and computation, chapter 4: Entanglement, 2001.
- [49] K. Onuma and A. Ito, Chemistry of Materials 10, 3346 (1998), http://dx.doi.org/10.1021/cm980062c.
- [50] A. Oyane, K. Onuma, T. Kokubo, and I. Atsuo, The Journal of Physical Chemistry B 103, 8230 (1999), http://dx.doi.org/10.1021/jp9910340.
- [51] A. Dey et al., Nat. Mat. 9, 1010 (2010).
- [52] G. Treboux, P. Layrolle, N. Kanzaki, K. Onuma, and A. Ito, The Journal of Physical Chemistry A 104, 5111 (2000), http://dx.doi.org/10.1021/jp994399t.
- [53] N. Kanzaki, G. Treboux, K. Onuma, S. Tsutsumi, and A. Ito, Biomaterials 22, 2921 (2001).
- [54] X. Yin and M. Stott, J. Chem. Phys. 118, 3717 (2003).
- [55] M. W. Swift, C. G. Van de Walle, and M. P. A. Fisher, Phys. Chem. Chem. Phys. 20, 12373 (2018).
- [56] M. Freedman, M. Shokrian-Zini, and Z. Wang, arXiv e-prints (2018), 1811.08580.
- [57] Y. Li, X. Chen, and M. P. A. Fisher, Phys. Rev. B **100**, 134306 (2019).
- [58] A. Chan, R. M. Nandkishore, M. Pretko, and G. Smith, Phys. Rev. B 99, 224307 (2019).

- [59] B. Skinner, J. Ruhman, and A. Nahum, Phys. Rev. X 9, 031009 (2019).
- [60] J. Martin and V. Vennin, Phys. Rev. D **96**, 063501 (2017).
- [61] B. Tsirelson, J. Sov. Math. **36**, 557 (1987).
- [62] L. J. Landau, Foundations of Physics 18, 449 (1988).
- [63] L. Masanes, arXiv e-prints, quant (2003), quant-ph/0309137.
- [64] S. Popescu and D. Rohrlich, Foundations of Physics 24, 379 (1994).
- [65] P. Janotta and H. Hinrichsen, Journal of Physics A: Mathematical and Theoretical 47, 323001 (2014).
- [66] M. Bock, A. Lenhard, C. Chunnilall, and C. Becher, Opt. Express 24, 23992 (2016).
- [67] Online code repository, https://github.com/aBeneWatts/macroscopic-bell.